

Material Matters™

Volume 9, Number 3

ALDRICH
Materials Science

Polymers in Therapeutics and Nanomedicine

The Future of Biomedicine— Delivered

POLY(AMINO ACID) BLOCK COPOLYMERS

FOR DRUG DELIVERY AND OTHER BIOMEDICAL APPLICATIONS

STIMULI-RESPONSIVE MATERIALS

AS INTELLIGENT DRUG DELIVERY SYSTEMS

ELECTROSPUN NANOFIBERS

FOR DRUG DELIVERY SYSTEMS

CHITOSAN: A VERSATILE PLATFORM

FOR PHARMACEUTICAL APPLICATIONS

Introduction

The third issue of *Material Matters*™ in 2014 is focused on Polymers in Therapeutics and Nanomedicine. This issue covers a variety of topics including synthetic and natural polymers that deliver a therapeutic payload using stimuli-response, self-assembly, or electrospun fibers.

The first article, by Carmen Scholz (USA), reviews poly(amino acid) block copolymers. These biocompatible polymers are inspired by the activity and capabilities of enzymes. By synthesizing PEGylated polymers using one or two amino acids, the resulting self-assembled polymeric micelles or membranes allow for drug delivery in a variety of configurations. They can also be used to enable attachment of a drug delivery system to a surface.

In our second article, Amit Singh and Mansoor M. Amiji (USA) review stimuli-responsive materials as intelligent drug delivery systems. There are a variety of smart materials that are able to be tuned to deliver a drug as a result of several different types of stimuli. Highlights include pH-, redox-, enzyme-, thermo-, light-, ultrasound-, magnetically, and electrically responsive polymers.

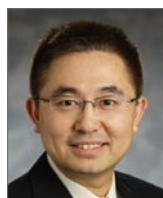
Sang Jin Lee, James J. Yoo, and Anthony Atala (USA), review electrospun nanoscale fibers used in drug or protein delivery systems in our third article. They highlight several different apparatus for electrospinning, as well as methods to control the fiber properties. The resulting scaffolds were shown to have the ability to deliver a variety of drugs and proteins in a controlled manner.

The fourth article, by Raphaël Riva and Christine Jérôme (Belgium), reviews chitosan as a platform for pharmaceutical applications. Chitosan is a natural polymer which can be used to encapsulate drugs and has been shown to improve the therapeutic efficiency and bioavailability, as well as enable targeted delivery. Specifically, chitosan has been used with difficult-to-deliver genes and hydrophobic drugs.

Each article in this issue is accompanied by a list of polymers available from Aldrich® Materials Science. Contact us at matsci@sial.com if you need any material that you cannot find in our catalog, or would like a custom grade for your development work. We welcome your new product requests and suggestions as we continue to grow our polymer offering.

About Our Cover

Polymers in therapeutics and nanomedicine allow for improved solubility, decreased toxicity, controlled release, and can help enable site-specific delivery. Polymers are used to generate numerous biomolecule-polymer conjugates, small molecule drug-polymer conjugates, supramolecular drug-delivery systems, and can be used as a platform for controlled release. This issue's cover art artistically illustrates a variety of drug-delivery systems, including functionalized multivalent polymer micelles, well-defined nanostructures, and polyplexes flowing through a blood vessel.



Yong Zhang, Ph.D.
Aldrich Materials Science

Material Matters™

Vol. 9, No. 3

Aldrich Materials Science
Sigma-Aldrich Co. LLC
6000 N. Teutonia Ave.
Milwaukee, WI 53209, USA

To Place Orders

Telephone 800-325-3010 (USA)
FAX 800-325-5052 (USA)

International customers, contact your local Sigma-Aldrich office (sigma-aldrich.com/worldwide-offices).

Customer & Technical Services

Customer Inquiries	800-325-3010
Technical Service	800-325-5832
SAFC®	800-244-1173
Custom Synthesis	800-244-1173
Flavors & Fragrances	800-227-4563
International	314-771-5765
24-Hour Emergency	314-776-6555
Safety Information	sigma-aldrich.com/safetycenter
Website	sigma-aldrich.com
Email	aldrich@sial.com

Subscriptions

Request your **FREE** subscription to *Material Matters*:

Phone	800-325-3010 (USA)
Mail	Attn: Marketing Communications Aldrich Chemical Co., Inc Sigma-Aldrich Co. LLC P.O. Box 2060 Milwaukee, WI 53201-2060
Website	aldrich.com/mm
Email	sams-usa@sial.com

Online Versions

Explore previous editions of *Material Matters* aldrich.com/materialmatters



Now available for your iPad®
aldrich.com/mm

Material Matters (ISSN 1933-9631) is a publication of Aldrich Chemical Co., Inc. Aldrich is a member of the Sigma-Aldrich Group.

©2014 Sigma-Aldrich Co. LLC. All rights reserved. SIGMA, SAFC, SIGMA-ALDRICH, and ALDRICH, are trademarks of Sigma-Aldrich Co. LLC, registered in the US and other countries. Material Matters is a trademark of Sigma-Aldrich Co. LLC. iPad is a registered trademark of Apple Inc. Pluronic is a registered trademark of BASF Corporation. RESOMER is a registered trademark of Evonik Roehm GMBH LLC. Sigma brand products are sold through Sigma-Aldrich, Inc. Purchaser must determine the suitability of the product(s) for their particular use. Additional terms and conditions may apply. Please see product information on the Sigma-Aldrich website at www.sigmaaldrich.com and/or on the reverse side of the invoice or packing slip.

Table of Contents

Articles

Poly(Amino Acid) Block Copolymers for Drug Delivery and Other Biomedical Applications	73
Stimuli-Responsive Materials as Intelligent Drug Delivery Systems	82
Electrospun Nanofibers for Drug Delivery Systems	89
Chitosan: A Versatile Platform for Pharmaceutical Applications	95

Featured Products

Triblock Copolymers A list of BAB triblock copolymers	77
Poly(ethylene glycol)s A selection of PEG-PCL diblock and PEG macroCTA polymers	77
Synthetic Poly(amino acid)s A list of synthetic homopolymers and copolymers	78
PolyNIPAMs A selection of polyNIPAMs and functionalized polyNIPAMs	86
Well-defined Biodegradable Polymers A selection of polylactides, end-functionalized poly(L-lactide)s, and block copolymers	92
Chitosans A list of chitosans from white mushroom and animal origins	98

Your Materials Matter



Bryce P. Nelson, Ph.D.
Aldrich Materials Science Initiative Lead

We welcome fresh product ideas. Do you have a material or compound you wish to see featured in the Aldrich® Materials Science line? If it is needed to accelerate your research, it matters. Send your suggestion to matsci@sial.com for consideration.

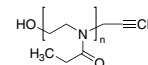
Professor Richard Hoogenboom at Ghent University (Belgium) has recommended the addition of functionalized poly(2-alkyl-2-oxazoline), or poly(2-oxazoline) polymers to our product portfolio for biomedical applications. This includes alkyne-terminated poly(2-ethyl-2-oxazoline) (Aldrich Prod. No. 778338). Poly(2-oxazoline) polymers demonstrate a lower critical solution temperature (LCST) behavior in aqueous solutions and can be used as thermo-responsive materials for biomedical applications because their transition temperatures are close to that of the human body.^{1,2,3} Poly(2-oxazoline) has also been used in various other bio-inspired methods and for polymer therapeutics.^{4,5} In particular, our alkyne-terminated clickable poly(2-oxazoline) products can be used as versatile building blocks for the construction of a large variety of complex, well-defined polymer architectures (including cyclodextrin core star-polymers) as well as virus and peptide polymer conjugates.^{1,6,7}

References

- (1) Chapman, R.; Bouten, P.J.M.; Hoogenboom, K.A.J.; Perrier, S. *Chem. Comm.* **2013**, 49, 6522.
- (2) Hoogenboom, R. *Angew. Chem. Int. Ed.* **2009**, 48, 7978–7994.
- (3) Hoogenboom, R.; Thijs, H.M.L.; Jochems, M.J.H.C.; van Lankvelt, B.M.; Fijten, M.W.M.; Schubert, U.S. *Chem. Commun.*, **2008**, 5758–5760.
- (4) Manzenrieder, F.; Luxenhofer, R.; Retzlaff, M.; Jordan, R.; Finn, M.G. *Angew. Chem. Int. Ed.* **2011**, 50, 2601–2605.
- (5) Hoogenboom, R.; Schlaad, H. *Polymers* **2011**, 3, 467–488.
- (6) Luxenhofer, R.; Han, Y.; Schulz, A.; Tong, J.; He, Z.; Kabanov, A.V.; Jordan, R. *Macromol. Rapid Commun.* **2012**, 33, 1613–1631.
- (7) Fijten, M.W.M.; Haensch, C.; van Lankvelt, B.M.; Hoogenboom, R.; Schubert, U.S. *Macromol. Chem. Phys.* **2008**, 209, 1887–1895.

Poly(2-ethyl-2-oxazoline), alkyne terminated

Polyethyloxazoline [1171957-24-6] $C_3H_5(C_2H_3NO)_nOH$



acetylene polyethyloxazoline 5kDa

▶ average M_n , 5,000, ≤ 1.2

powder

Store at: 2–8°C

778338-1G

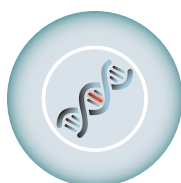
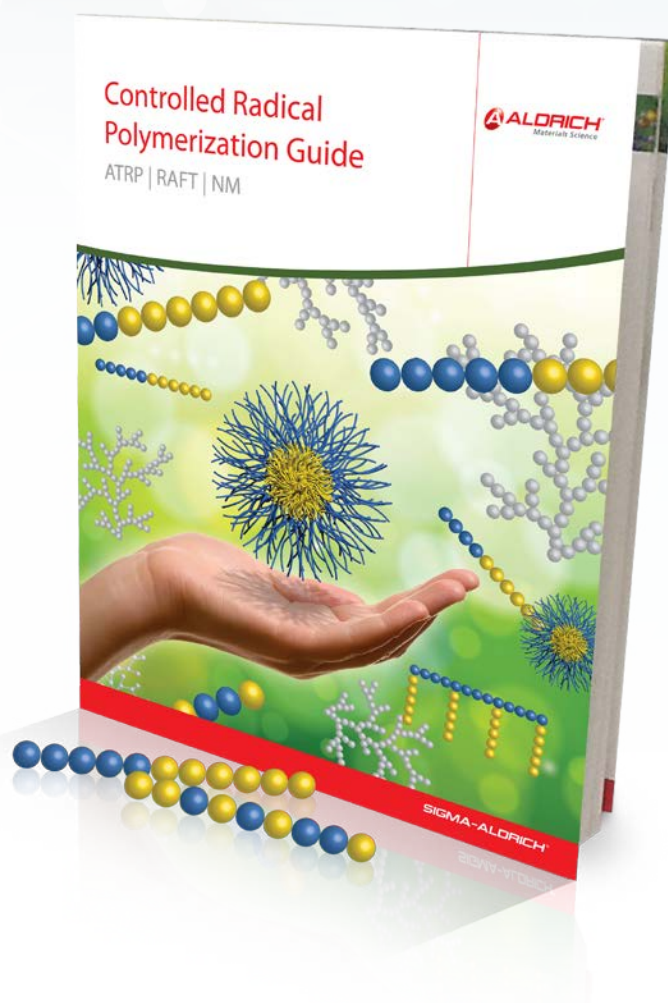
1 g

CONTROLLED RADICAL POLYMERIZATION GUIDE

Enabling Well-defined Copolymers

- Procedures written by CRP experts for different polymerizations. Authors include:
 - Edmondson
 - Haddleton
 - Matyjaszewski
 - Moad
 - Wooley
- Mini-reviews of the technology help determine:
 - The right techniques
 - The right reagents
 - The right conditions
- Controlled Radical Polymerization Tools:
 - New initiators
 - Reversible Addition/Fragmentation Chain Transfer (RAFT) agents
 - Atom Transfer Radical Polymerization (ATRP) ligands and monomers

Request your FREE CRP guide online at
aldrich.com/crpm



BIOMEDICAL



ELECTRONICS



ENERGY

POLY(AMINO ACID) BLOCK COPOLYMERS

FOR DRUG DELIVERY AND OTHER BIOMEDICAL APPLICATIONS



Carmen Scholz
Department of Chemistry, University of Alabama in Huntsville
Huntsville, AL 35899
Email: scholz@uah.edu

Introduction to Polyamino Acids: The Next Best Thing to Proteins

Humankind has utilized protein materials throughout its existence, starting with the use of materials such as wool and silk for warmth and protection from the elements and continuing with the use of recombinant DNA techniques to synthesize proteins with unique and useful properties. Proteins consist of amino acids linked in a pre-determined and genetically-prescribed sequence. There are twenty amino acids found in naturally occurring proteins. Commonly known as the standard proteinogenic amino acids, the sequence of these building blocks form the basis of protein function. The specific function of the protein impacts the sequence and abundance of particular amino acids. For example, the protection of the *Bombyx mori* pupa within the silk cocoon is a primary natural function of silk protein. As can be expected, the very hydrophobic and chemically non-reactive glycine and alanine comprise 70% of the amino acids in silk protein. Enzymes, however, are proteins that perform significantly different functions and, as such, are comprised of a different set of amino acids. Enzymes fulfill biochemical catalytic functions and their amino acid sequence enables catalytic activity through the composition and molecular architecture of the catalytic pocket. The stability of the enzyme is maintained via its unique tertiary structure and the solubility of the enzyme in its (aqueous) medium of activity is guaranteed by functionalized amino acids that form the outside of the three dimensional structure.

This capability to enable unique and highly-targeted biological function makes proteins ideal candidates for drug delivery systems because proteins have the ability to:

- Form an ideal “cradle” for a variety of therapeutic drugs, including delicate hydrophilic proteins or hydrophobic small molecules.
- Interact with, fold, and transport DNA.
- Deliver a therapeutic to a targeted location using site-specific interactions, exploit transmembrane transport mechanisms, and deliver a therapeutic payload to a specific site of action, free of side-effects.

However, our ability to engineer protein structure as well as understanding the infinite resulting interaction possibilities is still in its infancy. Despite of our current understanding of the intricacies of proteomics, the synthesis of fault-free (i.e., sequence-correct) proteins in appreciable amounts is still unresolved.

The limitations in our ability to synthesize proteins tailored for delivery of specific drugs has led researchers to concentrate on “the next best thing”: poly(amino acid)s (PAAs). While this category of polymers is also sometimes referred to as “polypeptides”, this author suggests the use of the term is slightly misleading because “peptide” refers to a polymeric structure with a specific amino acid sequence. However, in the macromolecules considered here, typically only two or three different amino acids are used for synthesis and no specific amino acid sequence is achieved.

PAAs are similar to proteins (and peptides) in that they consist of amino acid building blocks linked by means of amide bonds. This backbone architecture and the use of naturally occurring L-amino acids for their synthesis ensure their biocompatibility. Subsequently, their potential degradation products are L-amino acids, which will be readily absorbed by the body. Most PAAs consist of no more than two different amino acids that are linked to yield either random or block copolymers.

When L-amino acids are used in the synthesis of PAAs, the polymeric products retain the stereoregularity of the monomers. This results in the creation of isotactic PAA polymers. This is structurally very important as the stereoregularity is responsible for the formation of distinct secondary structures. Typically, helices are expected as secondary structures for isotactic polymers. The resulting PAA copolymers also exhibit the chemical characteristics of the L-amino acid building blocks, such as polarity, electrostatic, and solubility behavior. These physical characteristics are exploited when amphiphilic block copolymers are synthesized. Amphiphilic block copolymers readily undergo self-assembly into gels, micelles, membranes, vesicles, nanoparticles, nanogels, and other three-dimensional structures. The synthesis and utilization of PAA block copolymers is discussed in this article.

Synthesis of Poly(amino acid)s

Poly(amino acid)s and their syntheses were discussed in detail by Kricheldorf.¹ PAAs are typically synthesized by the ring-opening polymerization of amino acid *N*-carboxyanhydrides (NCAs) initiated by an amino-terminated reagent, as shown in **Figure 1**. Results indicate the polymerization follows a living, ring-opening polymerization. This polymerization technique allows for the synthesis of PAA block copolymers as well as random copolymers, making it highly versatile. If the amino acid NCAs are added successively to the initiator (the addition of the NCA of amino acid A followed by the addition of the NCA of amino acid B), AB block copolymers are formed. If the NCAs of the two amino acids are added to the initiator as a mixture, random copolymers are formed. Additional polymer architectures of varying complexity can be achieved due to the living nature of the polymerization.

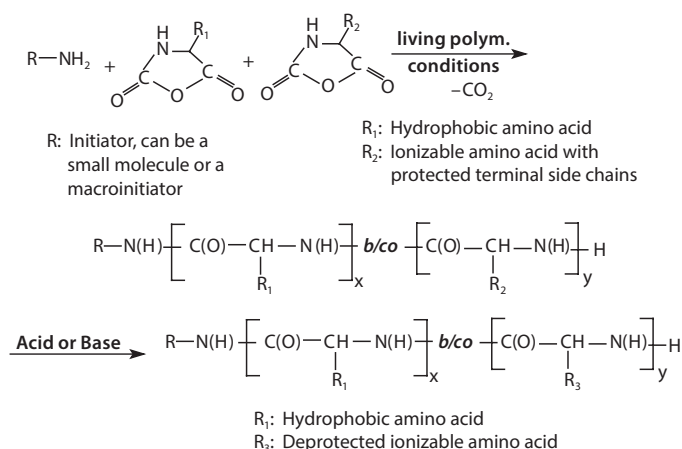


Figure 1. Schematic of NCA polymerization leading to the synthesis of PAA block copolymers and PAA random copolymers.

When synthesizing PAAs for drug delivery and biomedical applications, it is crucial to tightly control the molecular weight within a narrow range. This can be accomplished by employing living polymerization techniques to produce block copolymers. To do this, Hadjichristidis *et al.* employed high vacuum techniques to purify the monomers, solvents, and initiator. The polymerization was then performed in a specialized vessel that guaranteed absolutely anhydrous conditions.² Deming *et al.* developed syntheses that use transition metal catalysts to gain control over the molecular weight and polydispersity of the synthesized PAAs.³ Our own studies have shown that the first few addition reactions (i.e., the addition of the first few amino acid building blocks to the initiator) are most crucial to controlling the reaction and producing PAAs of the desired molecular weight and polydispersity.⁴ In the beginning of the polymerization, the nascent oligomers are not yet long enough to form a helical structure, but tend to form β -sheets due to strong hydrogen bond interactions. The rigidity of these structures suppresses the ability of the growing chain to undergo continued nucleophilic attacks on NCA monomers and these small β -sheet structures have a tendency to precipitate out of the polymerization solution, effectively stopping the polymerization.⁵ If the β -sheet formation is not kept under control, the resulting final product consists of a few long chains that exceed the intended chain length as determined by the Monomer:Initiator ratio and low molecular weight oligomers.

It was found that urea effectively suppresses the hydrogen bond formation between nascent PAA chains. As a result, the premature precipitation of product is suppressed. This allows for the polymerization to follow a living mechanism.⁴ Because urea suppresses the formation of β -sheets, there is sufficient time for the amino acid chains to reach a length of about 10 repeat units, enabling formation of α -helices. Once the β -sheet stage is overcome, polymerization proceeds in a controlled manner, where chain ends remain reactive (living) and block copolymers can readily form (**Figure 1**).

Poly(amino acid) Block Copolymers: Concepts for Drug Delivery Systems

Amino acids have diverse chemical properties and can be subdivided according to the nature of their side chains, including those that are aliphatic, aromatic, sulfur-containing, and those that contain ionizable groups. When designing a PAA for use in drug delivery, amino acids are selected based on chemical properties that meet the needs of both the drug and the solvent environment. Typically, amphiphilic block copolymers are formed from a hydrophilic (ionizable) and a hydrophobic amino acid (**Figure 1**). This amphiphilicity will induce self-assembly of the block copolymer when exposed to a selective solvent.⁶ In the case of drug delivery, where polymers are exposed to an aqueous environment, the hydrophilic segment of the block copolymer forms the outer layer or corona of the self-assembled structure, while the hydrophobic block self-assembles into a tightly packed structure that functions as a "cargo compartment" for hydrophobic drugs (**Figure 2A**).

Deming *et al.* studied the self-assembly and packing of PAA diblock and triblock copolymers and provided an excellent model to illustrate the polymer interactions and their subsequent self-assembly (**Figure 2**).⁷ Specifically, they studied copolymers consisting of poly(L-Leu), a hydrophobic amino acid and poly(L-Lys), an ionizable amino acid. Polymers of the following general structures were prepared: diblock copolymers: p(L-Lys)-*block*-p(L-Leu) and triblock copolymers: p(L-Lys)-*block*-p(L-Leu)-*block*-p(L-Lys), and individual blocks varied in length. The resulting block copolymers have a positively charged p(L-Lys) block that contributes to its solubility in water and where it forms a distorted (stretched) random coil. The hydrophobic p(L-Leu) block forms an α -helix as a secondary structure that is maintained when exposed to an aqueous environment. In the case of the triblock copolymers, there are two p(L-Lys) blocks that are adjacent to the p(L-Leu) block.

When used as drug delivery vehicles, amphiphilic diblock copolymers generally self-assemble into classic spherical polymeric micelles upon exposure to a selective solvent such as water (**Figure 2A**). In most cases, the hydrophobic segment packs tightly to avoid contact with the water and the hydrophilic segment readily solubilizes to form a shell or corona around the hydrophobic core. However, in the case p(L-Lys)-*block*-p(L-Leu) diblock copolymers the very stable p(L-Leu) helical structure, assembles into a stiff rod shape, which impedes the formation of a spherical packing structure and a flat lamellar packing of the rods (**Figure 2B**) predominates. The rods line up in parallel and are held in place through hydrophobic intermolecular interactions. However, the hydrophilic blocks with increasing chain lengths assume a stretched random coil configuration and fill increasing molar volumes. In addition, electrostatic repulsion between the positively charged p(L-Lys) chains renders the situation even more energetically unfavorable. As the chain length of the hydrophilic blocks increases, curved membranes are formed. These are the result of asymmetric packing of the hydrophilic blocks (**Figure 2C**). The resulting

increase in corona volume is energetically favorable. Structures with curvature in two directions can give rise to the formation of polymeric giant unilamellar vesicles. The repulsive effect between the p(L-Lys) blocks can also be resolved by twisting the plane of the p(L-Leu) blocks into fibrils, (Figure 2D). While the helices of the p(L-Leu) blocks maintain parallel packing, the hydrophilic blocks gain volume by expanding around the forming fibrils which extend in one direction only.

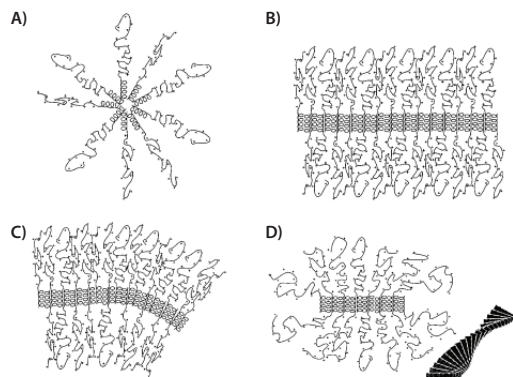


Figure 2. Self-assembly arrangement of PAA di- and triblock copolymers into (A) spherical micelles; (B) flat membranes; (C) curved membranes, and (D) fibrils, with the cross section extending out of the plane of the paper and the insert depicting how the helices assemble into twisted fibers. Reprinted with permission from Ref. 7, Copyright 2004, American Chemical Society.

In the case of p(L-Lys)-*block*-p(L-Leu)-*block*-p(L-Lys) triblock copolymers, where the two hydrophilic blocks are covalently attached to the hydrophobic core curved structures (Figure 2C) will not form. Instead, asymmetric packing of the p(L-Lys) blocks is impossible and fibrils readily form. Both the curved and the fibrillar structure models can be used to explain the gelation behavior observed for the p(L-Lys)-*block*-p(L-Leu) and p(L-Lys)-*block*-p(L-Leu)-*block*-p(L-Lys) block copolymers.⁸ Due to their amphiphilic nature, these copolymer systems can be readily loaded with hydrophobic (in the core) as well as hydrophilic (in the corona) drugs.

One can further expand on the above concept of PAA-based drug delivery systems, by using a macroinitiator to start the ring opening polymerization of amino acid NCAs. Poly(ethylene glycol) (PEG), is one of the most thoroughly investigated biocompatible polymers. With its large excluded volume, PEG conveys a “stealth character” to the structures to which it is attached. This essentially makes the structures “invisible” to adjacent protein molecules. The effectiveness of PEG to reduce protein interaction has been explained in physico-chemical terms by its low interfacial free energy in water and by its unique coordination with water molecules, as each PEG repeat unit coordinates with two to three water molecules. PEGylated PAA structures are used as drug delivery systems, employing polymeric micelles or nanoparticles with PEG to form the corona. They are also used to biocompatibilize surfaces of implantable devices intended to be in contact with protein-containing (bodily) fluids. In the case of drug delivery systems, PEGylation prevents uptake by the reticuloendothelial system and PEG-coated surfaces are efficient in suppressing biofouling.

The synthesis of PEGylated PAAs follows the scheme presented in Figure 1, with R representing NH₂-terminated PEG. For biomedical applications, PEGs with molecular weights of 2,000 to 10,000 Da are typically used to ensure renal clearance of degradation products. It is also possible to use bifunctional, α,ω -diamino PEGs as macroinitiators. The resulting block copolymers will have the PEG block in the middle, allowing the formation of interesting self-assembled molecular architectures, such as flower-like micelles.

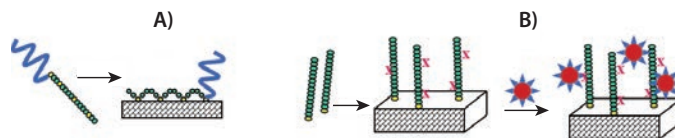


Figure 3. Surface modification with PEGylated PAA. A) The multi-point attachment of the PAA chain to the surface (e.g., by the formation of covalent bonds between L-Cys (yellow) and a gold surface) with the PEG-block (blue) extending away from the surface, thereby conveying a stealth character. B) Attachment of amino acid oligomers by single-point attachment and their subsequent modification with PAA-based polymeric micelles. The X indicates reactive terminal side groups, e.g., amino groups in L-Lys. A covalent bond is established between the PAA oligomer and the PAA polymeric micelle.

PEGylated PAAs can be attached directly to a surface and this surface attachment can be utilized for drug delivery applications.⁹ The attachment of PEGylated PAAs containing (L-Cys) repeat units can be achieved using gold-covered surfaces.¹⁰ To do this, L-Cys NCA is typically copolymerized with another amino acid (shown in green in Figure 3A), such as L-Lys NCA or L-Glu NCA, to achieve the optimal spacing (dilution) of the reactive L-Cys residues. The L-Cys repeat units react instantaneously with gold surfaces. The repeating L-Cys units in each block copolymer chain result in multiple anchor points to the surface (Figure 3A).

Because the PAA block functions as a multivalent anchor, the PEG block is free to extend away from the surface upon exposure to an aqueous environment. This architecture accomplishes two objectives: 1) PEG is strongly attached to the surface through multiple covalent thiol-gold linkages, and 2) the PAA block remains closely bound to the surface. These two factors contribute to the overall biocompatibility of the surface by masking “holes” that may form between individual PEG chains. It is well known the formation of dense polymer brushes is inherently difficult on surfaces using a “grafting to” method. This is because the concentration gradient built up by the already attached chains provides a strong kinetic hindrance against additional grafting. Furthermore, the large excluded volume that PEG exerts in an aqueous environment, while beneficial for preventing protein interactions, hinders the formation of dense PEG brushes in “grafting to” procedures even further. Figure 4 shows complete coatings are achieved on gold surfaces with both, PEG-*block*-p(L-Glu)₁₁₀-*block*-p(L-Cys)₁₀ and PEG-*block*-poly((L-Glu)₁₁₀-*co*-(L-Cys)₁₀). The polymer architecture, PAA random copolymer vs. block copolymer, has little to no influence on the polymer morphology on the surface. The coatings are homogenous and pinhole-free.

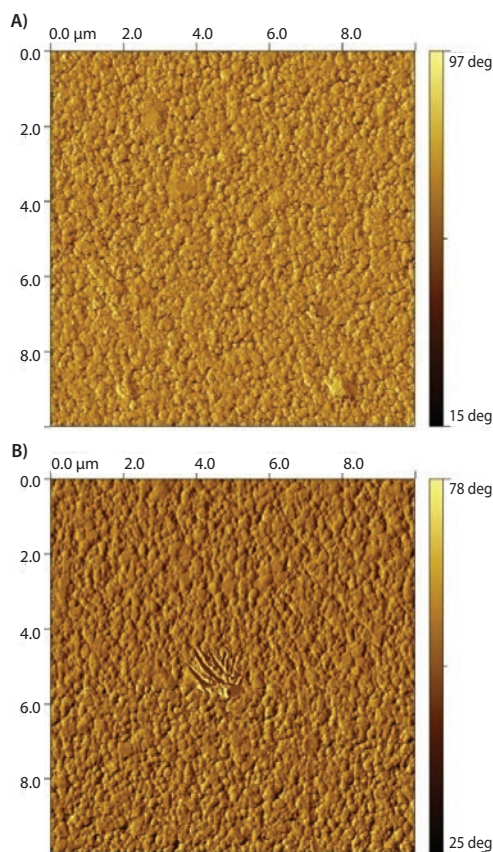


Figure 4. 10×10 μm AFM phase images of gold surfaces coated with PEG-*b*-p(L-Glu)₁₁₀-*block*-p(L-Cys)₁₀ (A) and PEG-*block*-p(L-Glu)₁₁₀-*co*-(L-Cys)₁₀ (B).

Another concept combines surface coating with the option of decorating the surface with PAA-based polymeric micelles that could be drug-loaded; the concept is schematically depicted in **Figure 3B**. In this procedure, oligo-(L-Lys) was attached covalently to the gold surface by a terminal thiol group, which is the result of using cysteamine as the initiator in the ring-opening polymerization of L-Lys NCA. Subsequently, the surface was decorated with micelles prepared from PEGylated PAAs (HOOC-CH₂-PEG₁₁₄-*block*-poly(Bz-L-Glu)₁₃) that carry carboxyl groups in their corona and were, therefore, reactive toward p(L-Lys).¹¹ Terminal carboxyl groups in the poly(Bz-L-Glu) side chains are protected as a benzyl ester to achieve the amphiphilicity that drives micellization. The resulting micelles are maintained due to the strong hydrophobic interaction of the benzyl groups in the micelle core. The micelles were covalently attached to the poly(L-Lys) using an amide linkage that formed between the terminal carboxyl groups of the polymeric micelles and the amino functions of poly(L-Lys), shown in **Figure 5**.

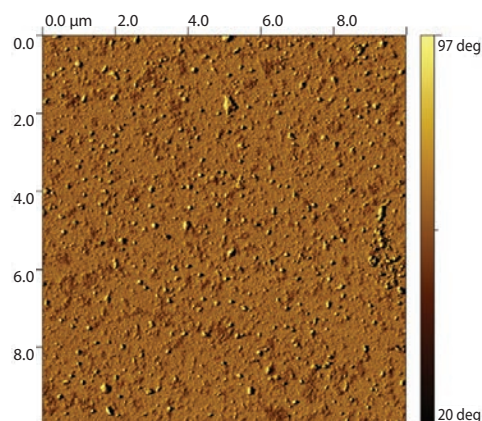


Figure 5. 10×10 μm AFM phase image of a gold surface coated with thiol-terminated p(L-Lys)₁₅ and decorated with polymeric micelles formed by HOOC-CH₂-PEG₁₁₄-*block*-p(Bz-L-Glu)₁₃.

Summary

The synthesis and application of PAA block copolymers in drug delivery and surface modification of biomedical products was discussed. Various self-assembly structures, including spherical polymeric micelles and membranes which enable gel formation, were examined. It was shown amino-terminated PEG can be used as a macroinitiator in the synthesis of PAAs, yielding block copolymers. PEGylated PAAs also self-assemble into polymeric micelles. Furthermore, if the PAA segment contains an amino acid that is reactive toward a surface (e.g., L-Cys reacts instantaneously with gold), the PAA *block* can be employed as a multi-point anchor to attach PEG covalently in a dense packing by a "grafting to" method to a surface. In a different surface modification approach, PAA oligomers attached covalently to a surface can be further decorated with PAA polymeric micelles, enabling attachment of a drug delivery system to a surface.

References

- (1) Kricheldorf, H.R. "Polypeptides" in: *Models of Biopolymers by Ring Opening Polymerization* (ed.: S. Penczek) CRC Press, Boca Raton, FL, **1990**, pp 3–132.
- (2) Hadjichristidis, N.; Iatrou, H.; Pispas, S.; Pitsikalis, M. *J. Polym. Sci., Part A: Polym. Chem.* **2000**, *38*(18), 3211–3234.
- (3) Deming, T.J. *JACS* **1997**, *119* (11), 2759–2760.
- (4) Ulkoski, D.; Armstrong, T.; Scholz, C. "Investigating the Secondary Structure of Poly(amino acids)" in: *Tailored Polymer Architectures for Pharmaceutical and Biomedical Applications* (ed. C. Scholz, J. Kressler) ACS Symposium Series 1135 **2013**, pp 69–85.
- (5) Komoto, T.; Kim, K.Y.; Oya, M.; Kawai, T. *Makromolekul. Chemie* **1974**, *175*(1), 283–299.
- (6) Kwon, G.S.; Kataoka, K. *Adv. Drug Delivery Rev.* **1995**, *16*, 295–309.
- (7) Breedveld, V.; Nowak, A.P.; Sato, J.; Deming, T.J.; Pine, D.J. *Macromolecules* **2004**, *37*, 3943–3953.
- (8) Deming, T.J. *Soft Matter*. **2005**, *1*, 28–35.
- (9) Guenther, M.; Gerlach, G.; Wallmersperger, T.; Avula, M.N.; Cho, S.H.; Xie, X.; Devener, B.V.; Solzbacher, F.; Tathireddy, P.; Magda, J.J.; Scholz, C.; Obeid, R.; Armstrong, T. *Adv. Sci. Technol.* **2013**, *85*, 47–52.
- (10) Obeid, R.; Armstrong, T.; Peng, X.; Busse, K.; Kressler, J.; Scholz, C. *Journal of Polymer Science, Part A, Polymer Science* **2014**, *52*(2), 248–257.
- (11) Obeid, R.; Scholz, C. *Biomacromolecules* **2011**, *12*(10), 3797–3804.

Triblock Copolymers

For more information on this product line, visit aldrich.com/block.

BAB Triblock Copolymers

Name	Structure	Molecular Weight	PDI	Degradation Time	Prod. No.
Poly(lactide- <i>block</i> -poly(ethylene glycol)- <i>block</i> -polylactide)		PEG average M_n 900 PLA average M_n 1,500 average M_n (1,500-900-1,500)	< 1.2 PDI	<12 months	659630-1G
Poly(lactide- <i>co</i> -glycolide)- <i>block</i> -poly(ethylene glycol)- <i>block</i> -poly(lactide- <i>co</i> -glycolide)		PEG average M_n 10,000 PLGA average M_n 2,200 average M_n (1,000-10,000-1,000)	< 2.0 PDI	2-3 weeks	764817-1G
Poly(lactide- <i>co</i> -caprolactone)- <i>block</i> -poly(ethylene glycol)- <i>block</i> -poly(lactide- <i>co</i> -caprolactone)		PEG average M_n 5,000 (DCM, PEO) PCL average M_n 5,700 average M_n (1,000-10,000-1,000)	< 1.3 PDI	1-2 months	764833-1G
Poly(lactide- <i>co</i> -glycolide)- <i>block</i> -poly(ethylene glycol)- <i>block</i> -poly(lactide- <i>co</i> -glycolide)		PEG average M_n 1,000 PLGA average M_n 2,000 average M_n (1,000-1,000-1,000)	< 1.2 PDI	1-2 weeks	764787-1G

Poly(ethylene glycol)s

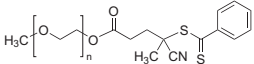
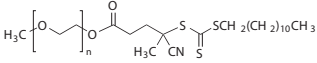
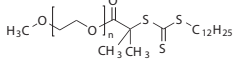
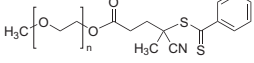
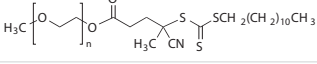
For more information on this product line, visit aldrich.com/peg.

PEG PCL Diblocks

Name	Structure	Molecular Weight	PDI	Degradation Time	Prod. No.
Poly(ethylene glycol)- <i>block</i> -poly(ϵ -caprolactone) methyl ether		PCL average M_n ~5,000 PEG average M_n ~5,000 average M_n ~10,000 (total)	< 1.4 PDI	>12 months	570303-250MG 570303-1G
Poly(ethylene oxide)- <i>block</i> -polycaprolactone, 4-arm		PCL average M_n ~2,500 PEG average M_n ~2,500 average M_n ~5,000 (total)	< 1.2 PDI	>12 months	570346-1G
Poly(ethylene glycol)- <i>block</i> -poly(ϵ -caprolactone) methyl ether		PCL average M_n ~13,000 PEG average M_n ~5,000 average M_n ~18,000 (total)	\leq 1.4 PDI	>12 months	570311-250MG 570311-1G
		PCL average M_n ~32,000 PEG average M_n ~5,000 average M_n ~37,000 (total)	< 1.4 PDI	>12 months	570338-250MG 570338-1G

PEG macroCTAs

Name	Structure	Molecular Weight	PDI	Prod. No.
Polystyrene, DDMAT terminated		average M_n 10,000	\leq 1.1 PDI	772569-1G
Poly(ethylene glycol) methyl ether 4-cyano-4-[(dodecylsulfanylthiocarbonyl)sulfanyl]pentanoate		average M_n 10,000	\leq 1.1 PDI	753033-1G
Poly(ethylene glycol) methyl ether (4-cyano-4-pentanoate dodecyl trithiocarbonate)		average M_n 5,400	\leq 1.1 PDI	751626-1G 751626-5G
Poly(ethylene glycol) methyl ether 2-(dodecylthiocarbonothioylthio)-2-methylpropionate		average M_n 5,000	\leq 1.1 PDI	736325-1G
Poly(ethylene glycol) methyl ether (2-methyl-2-propionic acid dodecyl trithiocarbonate)		average M_n 10,000	\leq 1.1 PDI	752495-1G

Name	Structure	Molecular Weight	PDI	Prod. No.
Poly(ethylene glycol) 4-cyano-4-(phenylcarbonothioylthio) pentanoate		average M_n 10,000	≤ 1.1 PDI	764930-1G
Poly(ethylene glycol) methyl ether (4-cyano-4-pentanoate dodecyl trithiocarbonate)		average M_n 2,400	≤ 1.1 PDI	751634-1G 751634-5G
Poly(ethylene glycol) methyl ether 2-(dodecylthiocarbonothioylthio)-2-methylpropionate		average M_n 1,100	≤ 1.1 PDI	740705-1G
Poly(ethylene glycol) 4-cyano-4-(phenylcarbonothioylthio) pentanoate		average M_n 2,000	≤ 1.1 PDI	764914-1G
Poly(ethylene glycol) methyl ether (4-cyano-4-pentanoate dodecyl trithiocarbonate)		average M_n 1,400	≤ 1.1 PDI	752487-1G 752487-5G

Synthetic Poly(amino acid)s

For more information on this product line, visit aldrich.com/polyaminoacid.

Homopolymers

Name	Molecular Weight	Prod. No.
Poly-L-histidine hydrochloride	≥ 5000	P2534-10MG P2534-25MG P2534-100MG P2534-500MG
Poly(γ -ethyl-L-glutamate)	$>100,000$	P8035-1G
Poly-L-proline	1,000-10,000	P2254-50MG P2254-100MG P2254-500MG P2254-1G
Poly-DL-lysine hydrobromide	1,000-4,000	P0171-100MG
Poly-D-lysine hydrobromide	1,000-5,000	P0296-10MG P0296-50MG P0296-100MG P0296-500MG P0296-1G
Poly-DL-alanine	1,000-5,000	P9003-25MG P9003-100MG P9003-1G
Poly-L-tryptophan	1,000-5,000	P4647-100MG
Poly-L-tyrosine	10,000-40,000	P1800-100MG
Poly-D-lysine hydrobromide	$\geq 300,000$	P1024-10MG P1024-50MG P1024-100MG P1024-500MG P1024-1G
Poly-L-lysine hydrochloride	15,000-30,000	P2658-25MG P2658-100MG P2658-500MG P2658-1G
Poly-L-ornithine hydrochloride	15,000-30,000	P2533-10MG P2533-50MG P2533-100MG P2533-500MG
Poly-L-lysine-FITC Labeled	precursor poly-L-lysine • HBr 15,000-30,000	P3543-10MG P3543-25MG
Poly-(α,β)-DL-aspartic acid sodium salt	2,000-11,000	P3418-100MG P3418-1G
Poly-D-glutamic acid sodium salt	2,000-15,000	P9917-100MG
Poly-DL-ornithine hydrobromide	3,000-15,000	P8638-25MG P8638-100MG P8638-250MG P8638-500MG
Poly- γ -benzyl-L-glutamate	30,000-70,000	P5011-500MG P5011-1G
Poly-DL-tryptophan	5,000-15,000	P8514-500MG

Name	Molecular Weight	Prod. No.
Poly-L-arginine hydrochloride	5,000-15,000	P4663-10MG P4663-50MG P4663-100MG
Poly-L-asparagine	5,000-15,000	P8137-25MG P8137-100MG
Poly-L-threonine	5,000-15,000	P8077-25MG P8077-100MG P8077-250MG
Poly (α,β -[N-(3-hydroxypropyl)-DL-aspartamide])	5,000-20,000	P0937-100MG
Poly-L-histidine	5,000-25,000	P9386-10MG P9386-50MG P9386-100MG
Poly- ϵ -Cbz-L-lysine	500-4,000	P4510-1G
Polyglycine	500-5,000	P8791-100MG P8791-500MG
Poly-L-glutamic acid sodium salt	750-5,000	P1943-100MG
Poly(L-lactide)	85,000-160,000	P1566-5G
Poly-L-lysine hydrochloride	>30,000	P9404-25MG P9404-100MG P9404-500MG P9404-1G
Poly-L-lysine, succinylated	>50,000	P3513-100MG P3513-1G
Poly-L-glutamic acid sodium salt	1,500-5,500	P1818-25MG P1818-100MG
Poly-DL-ornithine hydrobromide	15,000-30,000	P0421-100MG P0421-250MG
Poly-L-arginine hydrochloride	15,000-70,000	P7762-10MG P7762-50MG P7762-100MG
Poly-DL-lysine hydrobromide	25,000-40,000	P9011-25MG P9011-100MG
Poly-L-lysine-FITC Labeled	precursor poly-L-lysine • HBr30,000-70,000 30,000-70,000	P3069-10MG P3069-50MG
Poly-D-lysine hydrobromide	4,000-15,000	P6403-10MG P6403-50MG P6403-100MG
Poly-L-ornithine hydrobromide	5,000-15,000	P4538-10MG P4538-50MG P4538-500MG
Poly-L-lysine hydrobromide	500-2000	P8954-25MG P8954-100MG P8954-500MG
Poly- γ -benzyl-L-glutamate	70,000-150,000	P5386-100MG P5386-1G
Poly(D,L-lactide)	75,000-120,000	P1691-1G P1691-5G
Poly-DL-ornithine hydrobromide	>30,000	P0671-25MG P0671-100MG P0671-500MG
Poly-L-proline	>30,000	P3886-500MG P3886-1G
Poly-DL-lysine hydrobromide	>40,000	P4158-25MG P4158-100MG P4158-500MG
Poly-L-arginine hydrochloride	>70,000	P3892-10MG P3892-50MG P3892-100MG
Poly-L-lysine hydrobromide	1,000-5,000	P0879-25MG P0879-100MG P0879-500MG P0879-1G
Poly-D-glutamic acid sodium salt	15,000-50,000	P4033-10MG P4033-100MG P4033-1G
Poly-L-tryptophan	15,000-50,000	P4772-100MG
Poly- γ -benzyl-L-glutamate	150,000-350,000	P5136-1G
Poly-L-glutamic acid sodium salt	3,000-15,000	P4636-25MG P4636-100MG P4636-500MG P4636-1G

Name	Molecular Weight	Prod. No.
Poly-L-ornithine hydrobromide	30,000-70,000	P3655-10MG P3655-50MG P3655-100MG P3655-500MG P3655-1G
	>100,000	P4638-10MG P4638-50MG P4638-100MG P4638-500MG P4638-1G
Poly-L-glutamic acid sodium salt	15,000-50,000	P4761-25MG P4761-100MG P4761-500MG P4761-1G
Poly-D-lysine hydrobromide	30,000-70,000	P7886-10MG P7886-50MG P7886-100MG P7886-500MG P7886-1G
Poly-L-lysine hydrobromide	15,000-30,000	P7890-25MG P7890-100MG P7890-500MG P7890-1G
Poly-L-glutamic acid sodium salt	50,000-100,000	P4886-25MG P4886-100MG P4886-500MG P4886-1G
	>50,000	G0421-25MG G0421-100MG G0421-1G
Poly-L-lysine hydrobromide	30,000-70,000	P2636-25MG P2636-100MG P2636-500MG P2636-1G
Poly-D-lysine hydrobromide	70,000-150,000	P0899-10MG P0899-50MG P0899-100MG P0899-500MG P0899-1G
Poly-D-lysine hydrobromide	150,000-300,000	P1149-10MG P1149-100MG P1149-500MG
Poly-L-lysine hydrobromide	40,000-60,000	P3995-500MG P3995-1G
	70,000-150,000	P1274-25MG P1274-100MG P1274-500MG P1274-1G
Poly-L-glutamic acid sodium salt	50,000-100,000	81328-100MG
Poly-L-lysine hydrobromide	150,000-300,000	P1399-25MG P1399-100MG P1399-500MG P1399-1G
Poly-D-lysine hydrobromide	30,000-70,000	81358-500MG
Poly-L-lysine hydrobromide	≥300,000	P1524-25MG P1524-100MG P1524-500MG P1524-1G
	4,000-15,000	81331-50MG 81331-250MG
	20,000-30,000	81333-50MG 81333-250MG
	30,000-70,000	81338-250MG
	70,000-150,000	81339-25MG 81339-100MG
	≥300,000	81356-100MG 81356-500MG

Copolymers

Name	Molecular Weight	Feed Ratio	Prod. No.
Poly(Arg, Pro, Thr) hydrochloride	10,000-30,000	Arg:Pro:Thr (6:3:1)	P9431-25MG
Poly(Ala, Glu, Lys, Tyr) hydrobromide	20,000-30,000	Ala:Glu:Lys:Tyr (6:2:5:1)	P1152-10MG P1152-25MG
Poly(D-Glu, D-Lys) hydrobromide	20,000-50,000	D-Glu:D-Lys (6:4)	P7658-25MG P7658-100MG
Poly(Glu, Ala) sodium salt	20,000-50,000	Glu:Ala (6:4)	P1650-100MG
Poly(Glu, Ala, Tyr) sodium salt	20,000-50,000	Glu:Ala:Tyr (6:3:1)	P3899-25MG P3899-100MG
Poly(Glu, Lys, Tyr) sodium salt	20,000-50,000	Glu:Lys:Tyr (6:3:1)	P4409-10MG P4409-25MG P4409-500MG
Poly(Lys, Phe) 1:1 hydrobromide	20,000-50,000	-	P3150-10MG P3150-25MG P3150-100MG P3150-500MG
Poly(Lys, Tyr) hydrobromide	20,000-50,000	Lys:Tyr (4:1)	P4659-10MG P4659-25MG P4659-250MG
Poly(Glu, Tyr) sodium salt	5,000-20,000	Glu:Tyr (4:1)	P7244-25MG P7244-250MG
Poly(Glu, Lys) hydrobromide	75,000-125,000	Glu:Lys (1:4)	P8619-100MG
Poly(Glu, Tyr)-Agarose	-	Glu:Tyr (4:1)	P6835-5ML
Poly(Glu, Lys) hydrobromide	150,000-300,000	Glu:Lys (1:4)	P0650-100MG
Poly(Glu, Ala, Tyr) sodium salt	20,000-50,000	Glu:Ala:Tyr (1:1:1)	P4149-10MG P4149-25MG
Poly(Glu, Tyr) sodium salt	20,000-50,000	Glu:Tyr (4:1)	P0275-10MG P0275-25MG P0275-100MG P0275-250MG P0275-500MG
Poly(Arg, Pro, Thr) hydrochloride	5,000-20,000	Arg:Pro:Thr (1:1:1)	P9306-25MG
Poly(Lys, Tyr) hydrobromide	50,000-150,000	Lys:Tyr (1:1)	P4274-100MG
Poly(Glu, Glu-OEt)	70,000-150,000	Glu:Glu-OEt (1:1)	P4785-250MG
Poly(Glu, Tyr) sodium salt	20,000-50,000	Glu:Tyr (1:1)	P0151-25MG
	20,000-50,000	-	81357-50MG
Poly(D,L-lactide-co-glycolide)	66,000-107,000	lactide:glycolide (75:25)	P1941-1G P1941-5G

STIMULI-RESPONSIVE MATERIALS

AS INTELLIGENT DRUG DELIVERY SYSTEMS



Amit Singh and Mansoor M. Amiji*
 Department of Pharmaceutical Sciences, School of Pharmacy
 Northeastern University, Boston, MA 02115 USA
 *Email: m.amiji@neu.edu; Tel: 617-373-3137

Introduction

Materials science has revolutionized the central paradigm of drug delivery, especially for cancer therapeutics, such that the physicochemical properties of the delivery system can be customized to develop so-called *smart* or *intelligent* systems that can deliver the therapeutic molecule on-demand. Much of the advances in the design of materials for drug delivery has been inspired by a growing understanding of tumor microenvironments and the exploitation of the subtle differences in the tumor bio-milieu. Cancer is a complex disease involving many different cell types, extracellular matrices, immune factors, signaling molecules, and physiological phenomena. The significant diversity of the cell types involved in cancer poses a significant challenge for targeting a tumor with a therapeutic drug. Acquired multidrug resistance (MDR) to existing chemotherapies further compounds the problem, inevitably leading to poor clinical outcomes. The tumor microenvironment is remarkably diverse; it is characterized by a variety of characteristics, including abnormal tumor vasculature, absence of lymphatic drainage, hypoxia, lower pH gradient, redox environment, high interstitial pressure, and high protease activity.¹ At the cellular level, the tumor is comprised not only of cancer cells but also a diverse population that includes stromal cells, endothelial cells, components of immune cells, and cancer stem cells (CSCs).² These heterogeneities within the tumor impart survival advantages and promote tumor growth, and also help to progress and disseminate the disease to distant sites. Alternatively, subtle differences in tumor physiology can be used to stimulate a response using a smart polymer system, enabling the design of therapeutic strategies with tumor specificity.

Internally Regulated Systems

Internally regulated vectors (also known as *self-regulated* or closed-loop systems) respond to a stimulus from within the body such as pH, redox, presence of proteases, or other factors to regulate drug release. Change in the bio-milieu at the diseased site triggers a chemical or physical change in the delivery system, which leads to the release of the payload. The release profile is entirely dependent on the physiological status of the site of the disease and cannot be modulated externally.

pH-Responsive Systems

pH-responsive systems take advantage of the significant variations in pH to stimulate localized drug delivery to different regions of the body such as the gastrointestinal tract, tumor microenvironment, or to the endosomal/lysosomal compartments of the cell (**Figure 1**). Cancer cells prefer aerobic glycolysis as their primary source of energy irrespective of the oxygen concentration. This leads to accumulation of lactate in the tumor microenvironment which lowers the pH in the extracellular matrix. This phenomenon is often referred to as the “Warburg effect”. This not only serves the incessant demand for energy of a rapidly dividing cancer cell but also supplies the essential precursors for other macromolecule biosynthesis.⁴ pH-responsive vectors are typically designed using polymers that contain ionizable weak acids or weak bases to exploit the acidic microenvironment for controlled drug delivery into the tumors. These materials depend on protonation and deprotonation for the selective solubility in aqueous media. Acrylic acid (AAc) (**Aldrich Prod. No. 147230**), methacrylic acid (MAAc) (**Aldrich Prod. No. 155721**), maleic anhydride (MA) (**Aldrich Prod. No. M188**), *N,N*-dimethylaminoethyl methacrylate (DMAEMA) and 2-(methacryloyloxy)ethyl dihydrogen phosphate are some examples of weak acids and their derivatives that have been explored while poly(amidoamine) (PAA or PAMAM) is a common example of a polymeric weak base that has been extensively used for the design of pH-responsive delivery vectors. Poly(β -aminoester) (PbAE) is another polymer that possesses strong pH dependent solubility and PbAE has also been used in the design of pH-responsive delivery systems. A comprehensive *in vitro* and *in vivo* study using pH-responsive poly(ethylene oxide)-PbAE (PEO-PbAE) copolymer system demonstrated higher apoptosis in MDA-MB-231 breast cancer cells and effectively accumulated into the SKOV3 human ovarian cancer xenograft model.⁵⁻⁷ Several pH-responsive vectors have been suitable for delivery of biologics such as gene, siRNA, miRNA, peptides and proteins as well, which demonstrated the versatility of the delivery system.^{8,9}

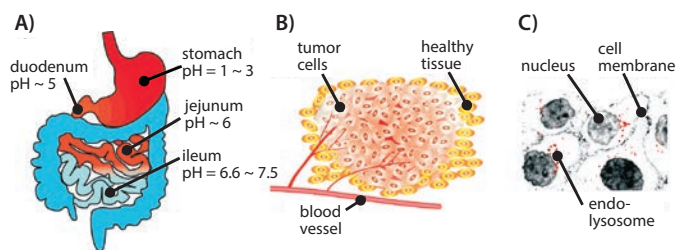


Figure 1. Schematic representation of differential pH environment at the organ (A), tissue (B), and cellular (C) level that could be exploited by pH-responsive drug delivery systems. Reprinted with permission from Reference 8, American Chemical Society 2010.

Redox-responsive Systems

Tumors exhibit characteristic oxidizing extracellular and reducing intracellular environments generating a redox potential that has become the driving force for the development of redox-responsive delivery vectors. Redox-responsive systems tend to lose their structural integrity in response to the significantly higher cytosolic and nucleus concentration of glutathione tripeptide (2–10 mM) compared to the extracellular matrix (2–20 μ M). Due to this response, disulfide bonds (S–S) are the most studied redox-sensitive linkage used to develop polymer-, lipid- or protein-based delivery systems. Shell shedding copolymers such as PEG-S-S-poly(ϵ -caprolactone) (PEG-S-S-PCL), PCL-S-S-poly(ethyl ethylene phosphate) (PCL-S-S-PEEP), S-S-PAA-g-PEG, or dextran-S-S-PCL have been successfully employed as redox-responsive delivery systems with faster drug delivery kinetics. This improvement is evident by the *in vitro* activity of the payload and excellent *in vivo* tumor growth regression.¹⁰ Our group has developed a thiolated gelatin-based protein nanoparticle system that demonstrated tremendous capability in delivering both small molecules and genes for targeting pancreatic cancer cells in pancreatic human adenocarcinoma bearing tumor xenografts.¹¹ In a separate study, these nanoparticles were loaded with plasmid encoding vascular endothelial growth factor (VEGF-1) in an orthotopic MDA-MB-231 human breast adenocarcinoma model which resulted in reduced tumor growth as well as angiogenesis.¹² Adopting a layer-by-layer (LbL) assembly approach, poly(vinylpyrrolidone) (PVP) (Aldrich Prod. No. 81430) coated on silica nanoparticles was used as a sacrificial template to form disulfide crosslinked poly(methacrylic acid) (PMA) capsules for use in the delivery of proteins and peptides for use as vaccines and as small-molecule anticancer drugs.¹⁰

Enzyme-responsive Systems

Proteases are an integral part of tumor physiology. Cancer-associated proteases (CAPs) such as matrix metalloproteinases (MMPs), cathepsins, and urokinase plasminogen activators (uPAs) play a crucial role in tumor tissue remodeling and in disease progression, invasion, and dissemination. MMPs have been shown to be overexpressed in a majority of cancers and are generally accepted to be important contributors to cancer progression and invasiveness.¹³ As a result, enzyme-responsive vectors have been designed with an enzyme-specific peptide in order to trigger delivery when the substrate is degraded by the enzymatic activity within the tumors. One example of these specially designed enzyme-responsive vectors was the local delivery of chemotherapeutic drugs by application of a protease sensitive matrix. Cisplatin conjugated to a protease cleavable peptide CGLDD was further bound to a PEG-diacrylate hydrogel wafer. This approach resulted in prompt drug release in response to the presence of MMP-2 or MMP-9. Dextran-PVGLIG-methotrexate conjugate showed a similar response from the MMPs to release the drug and demonstrated tumor inhibitory effect *in vivo*.¹⁴ 1,2-dioleoyl-*sn*-glycero-3-phosphoethanolamine (DOPE) (Sigma Prod. No. 76548) with acetylated dipeptide (N-Ac-AA) along with dioleoyl trimethylammonium propane (DOTAP) and phosphatidylethanolamine (PE) has been used to make non-fusogenic liposomes that turn fusogenic when activated by elastase or proteinase K, thereby improving the intracellular uptake.¹⁴

In a similar approach, DOPE functionalized with PEG using a protease responsive linker (e.g., GPLGIAGQ) was blended with distearyl phosphatidylcholine (DSPC), cholesteryl chloroformate, and cholesterol-5-yloxy-N-(4-((1-imino-2-, β -D-thiogalactosyl ethyl)amino)butyl) formamide (Gal-C4-Chol) to make liposomes with galactose on the surface for targeting hepatic cells. These galactose moieties are shielded by bulky PEG groups, which limit their uptake. However, in the presence of MMP-2, the peptide that links PEG to the liposomal surface is cleaved to expose the targeting ligand, facilitating their rapid uptake.¹⁴ In a more recent effort, a cholesterol-anchored graft polymer containing peptide GSGRSAGK (bearing consensus sequence for uPA) and acrylic acid was incorporated in liposomes made using

1,2-dioleoyl-*sn*-glycero-3-phosphocholine (DOPC, Sigma Prod. No. P6354), 1,2-dipalmitoyl-*sn*-glycero-3-phosphocholine (DPPC, Sigma Prod. No. P0763), and cholesterol (47.5:5:47.5 respectively) (Figure 2A). These liposomes with crosslinked polymers showed improved stability with resistance to osmotic swelling or leaking. In the presence of the enzyme, the crosslinking rapidly degraded; this caused drug release through swelling of the liposome (Figure 2B).¹⁵ Though the clinical application of these nanovectors is yet to be established, preclinical studies indicate that these systems hold tremendous promise in augmenting therapeutic efficacy of drugs that otherwise show poor bioavailability.

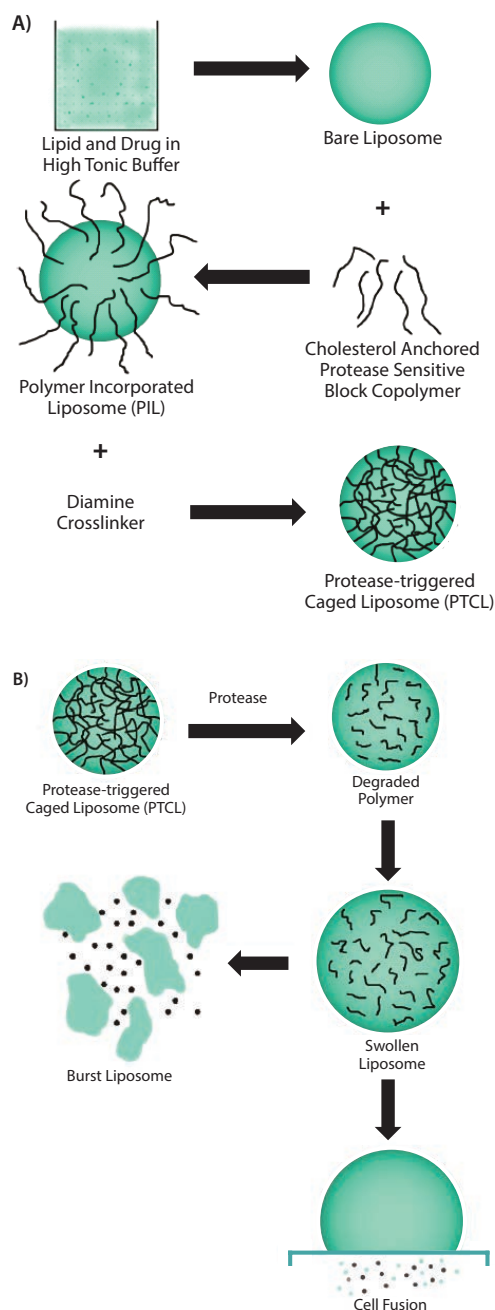


Figure 2. A) Scheme showing the multiple steps involved in the synthesis of uPA-sensitive, polymer-caged liposomes. B) Proposed mechanism of action of the polymer-caged liposomes in response to presence of enzyme. Reprinted with permission from Reference 15, American Chemical Society 2011.

Externally Regulated Systems

Externally regulated systems, also referred to as open-loop systems, are vectors whose drug delivery capability can be governed by a stimulus from outside the body. Since the duration and strength of the external stimulus can be precisely controlled, the drug release profile of these nanovectors can be temporally and spatially controlled to achieve an on-demand supply of the drug at a desired dose. Heat, light, sound, magnetic, and electrical stimuli have all been explored and are discussed below.

Thermo-responsive Systems

Thermo-responsive materials undergo a phase change below or above a particular temperature. These changes are referred to as lower or upper critical solution temperature (LCST or UCST), respectively. Such materials are insoluble above or below the critical temperature but transform to a completely soluble form upon crossing the transition temperature. Poly(*N*-isopropyl acrylamide) (PNIPAAm) is one such polymeric material that is not ideal for drug delivery applications. PNIPAAm becomes hydrophobic at 32 °C in water and at temperatures that are similar to physiological conditions. However, altering the side chains, the molecular weight of the polymer, the polymeric architecture, or copolymerizing with other hydrophilic or hydrophobic polymers enables customization of the transition temperature to suit biomedical applications. PNIPAAm derivative, therefore, have been explored extensively as a material for thermo-sensitive drug delivery vectors and have been incorporated into micelles, liposomes, hydrogels and nanogels, polymersomes, interpenetrating networks, films, and the surface of inorganic nanoparticles.¹⁶ Copolymers of PNIPAAm with poly(*N,N*-diethylacrylamide) (PDEAAm), poly(*N*-vinylcaprolactone) (PVCL), PLGA, poly[2-(dimethylamino) ethyl methacrylate] (PDMAEMA), PEG, gelatin, and chitosan have been used for the delivery of chemotherapeutic drugs and biologics. Beside drug delivery, considerable efforts have been made to develop thermo-sensitive materials for use in other applications including surfaces and scaffolds for tissue growth and engineering, imaging, and diagnostics.¹⁷

Light-responsive Systems

Light is a popular choice as an external stimulus since its intensity and penetration depth can be precisely controlled. As a result, light-sensitive materials have become increasingly popular as drug delivery systems. Azobenzene, *o*-nitrobenzene, coumarin, and pyrene derivatives are routinely used for devising light-responsive drug delivery vectors. Jiang et al. developed a UV-responsive micelle system with poly(ethylene oxide) (PEO) and poly(methacrylate) which included pyrene sidechains as diblock copolymers. The authors used Nile red dye (Sigma Prod. No. 19123) as a surrogate to demonstrate the efficient release of the payload as a function of irradiation time and illumination power.¹⁸ UV-irradiation, however, is not conducive for biological applications, especially for prolonged periods. For this reason, alternative materials responsive to visible or NIR wavelengths are being explored. Inorganic nanomaterials, especially anisotropic noble metal nanoparticles, show excellent NIR absorption characteristics and have been used as light-absorbing materials to facilitate drug delivery. Kang et al. used silica-coated gold nanorods with strong absorption maxima around 850 nm as a template to polymerize crosslinked acrylamide on the surface of the nanoparticle. Doxorubicin (DOX) loaded particles showed enhanced cell cytotoxicity upon irradiation with NIR light (808 nm) but the nanoparticles that had not been irradiated or irradiation in the absence of nanoparticles

showed little effect. These results confirmed light-mediated payload release.¹⁸ In a similar approach, Hribar, *et al.* developed a polymer-gold nanorod composite that allowed a controlled and precise release of small molecules (<800 Da) upon irradiation with NIR-light. The PbAE macromolecules (A6), *tert*-butyl acrylate (tBA) monomers, and 2-hydroxyethyl acrylate (10:20:70% w/w, respectively) were polymerized to form the polymer blend. A high concentration of gold nanorods and light-responsive material could then be loaded in the core of the polymer microparticles (Figure 3A–4C). *In vitro* release of loaded DOX demonstrated a strong dependence on the light irradiation (Laser ON) (Figure 3D) and generated increased toxicity in T6–17 cells due to light-induced drug release (Figure 3E).¹⁹

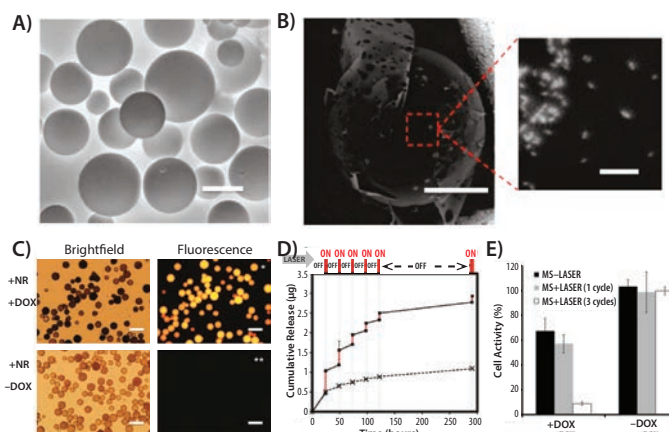


Figure 3. A) Environmental scanning electron micrograph of polymeric microspheres (MS) made of A6:HEA:tBA (10:20:70). The scale bar corresponds to 50 µm. B) Backscattered micrograph of the microsphere showing the embedded gold nanorods (bright spots, scale bar = 20 µm) and a magnified image of the highlighted area showing the nanorods within the microsphere (scale bar = 200 nm). C) Bright field and fluorescence images of the microsphere showing the microspheres. The DOX loaded microspheres show intense fluorescence (top panel, right) while those without DOX do not show any background fluorescence (bottom panel, right). Scale bar in all images corresponds to 100 µm. D) Cumulative drug release from the microspheres as a function of laser pulse (Wavelength = 808 nm) applied at physiological temperature (37 °C). E) Histogram plot of T6–17 cells activity after exposure to MS alone with laser and DOX-loaded MS with a laser pulse of 1 and 3 cycles (Laser power = 1.1 W, 5 min/cycle). Reprinted with permission from Reference 19, American Chemical Society 2011.

Ultrasound-responsive Systems

The intensity of ultrasound energy such as light can be tailored for its intensity and focused over a small area in the body. This maximizes the drug release efficiency and, therefore, is often referred to as high intensity focused ultrasound (HIFU). Due to its wide application in clinical imaging and diagnosis, ultrasound-based on-demand drug releasing vectors are seen as a natural material for the development of “theranostic” delivery systems. Ultrasound energy mediates drug release from a delivery vector by three main mechanisms: (1) heat generation, (2) acoustic cavitation, and (3) acoustic radiation forces. Some of the important parameters which can influence the performance of ultrasound-based techniques include the time and nature of application. The rationale behind ultrasound-based delivery is largely regulated by heat generation; therefore, the nanoparticle delivery systems designed for ultrasound-based delivery are similar in composition to thermo-responsive systems. Microbubble technology, initially developed for contrast enhancement in ultrasound imaging, has since been exploited for acoustic cavitation to alter cell permeability and has also been used as a delivery vehicle.²⁰

Ibsen, *et al.* prepared nested liposomes synthesized by a method in which a microbubble was created within the liposome to impart ultrasound-responsiveness and demonstrated that it could be used for delivery of both small and large molecules. Similarly, mRNA-lipoplex loaded microbubbles were employed as a vaccine to successfully transfect and express the reporter gene in dendritic cells. This led to a slight shift in maturation and, in turn, induced T-cell response.²¹ As a result, ultrasonic-assisted delivery is an attractive approach with significant potential.

Magnetically Regulated Systems

Like thermo- and ultrasound-responsive vectors, delivery systems responsive to magnetic fields rely on the induction of hyperthermia to release the payload. The ability to direct and concentrate these vectors in a specific area of the body through the application of an external magnetic field gives an added advantage to such delivery systems. Traditionally, magnetic nanoparticles such as superparamagnetic iron oxide nanoparticles (SPIONs) are incorporated into polymeric, lipidic, or protein delivery systems to impart them with magnetic properties. SPIONs have also been extensively used as magnetic resonance imaging (MRI) contrast agents, and their presence in a delivery vector offers an imaging modality that possesses stimuli-responsiveness. SPIONs coated with the thermo-responsive polymer PNIPAAm and loaded with DOX showed a rapid drug release above the lower critical solution temperature (LCST) due to magnetic field induced hyperthermia but a slow sustained release below the LCST. *In vivo* studies in buffalo rats implanted with hepatocellular carcinoma revealed magnetically guided increased accumulation and drug release in tumors. This resulted in an improved contrast-based MR imaging and efficient therapeutic potential.²² Majewski, *et al.* demonstrated the utility of the magnetically active vectors as a gene delivery system. Most importantly, the study demonstrated that internalized magnetic nanoparticles can be used for selective isolation of the transfected cells from the population.²³ Due to the added versatility of the magnetically regulated delivery system, they are now often used to design dual and multiple stimuli-responsive vectors to harvest the benefits of individual stimuli-responsiveness.²⁴

Electro-responsive Systems

Certain materials (organic and inorganic) exhibit conductive properties and can be used to design delivery systems that are responsive to an external electric field. Common examples of electro-sensitive materials for drug delivery include polypyrrole (PPy, Aldrich Prod. No. 577030), ferrocene, and carbon nanotubes. Weak electric pulses (~1 V) are generally used for such applications and these electric fields are preferred over other externally applied stimuli due to several advantages: an electric pulse is (1) easy to control and apply, (2) does not need sophisticated and elaborate instrumentation, and (3) can be easily integrated to design chip-based devices. Ge, *et al.* prepared dodecyltrimethylammonium bromide (DTAB) micelles with decyl alcohol as a cosurfactant, and PPy was polymerized in the hydrophobic core. These nanoparticles were then loaded with a thermo-sensitive PLGA-PEG-PLGA block polymer that showed temperature-dependent sol-gel transformation. The polymer exists as a solution at 4 °C but rapidly forms a gel at a physiological temperature of 37 °C. Daunorubicin and fluorescein were loaded into the nanoparticles that were embedded in the polymer matrix. The resulting material maintained its solid hydrogel form at body temperature and demonstrated an electric-pulse dependent drug release. The subcutaneously injected, soluble form rapidly forms a gel in FVB mice and successfully released the payload *in vivo* upon application of the electric

pulse. In the control group, the absence of an external stimulus resulted in insignificant release of the cargo.²⁵ Adopting a novel approach, Zhu, *et al.* grafted 4-(3-cyanophenyl) butylene (CPB) as an electric field-active “nanoimpeller” onto the wall of mesoporous silica. Due to their large inherent dipole moment, the grafted CPBs reorient under the influence of an applied electric field. The CPBs then rapidly release the guest molecules (ibuprofen) from their pores.²⁶

Future Perspectives

The plethora of available literature on stimuli-responsive delivery systems demonstrates the growing importance for these systems. However, a majority of these systems have not made it past the pre-clinical stage and only a handful of examples currently have entered clinical trials.²⁷ The need for a precise control over the “response” to the applied “stimulus” makes their clinical translation challenging. The complex synthetic steps and formulation of multiple components further compounds the issue. The majority of stimuli-responsive delivery systems are still in the early stages of development and the optimization of the synthesis procedures is needed before they can transition into the clinical world. Accuracy and precision over the stimulus will also need improvement from preclinical to the clinical level. Externally applied “physical” stimuli are easy to control and manipulate but internal “biological” triggers are not as easily controlled. Tumors show considerable variation in their physiological status between patients, organs, or even the same tumors in different species. External stimuli, on the other hand, need improvement to achieve better tissue penetration without causing any damage, which would require the optimization of several contributing parameters.

Other factors can also have a negative impact on delivery systems for the stimuli-responsive vectors. The EPR effect that leads to accumulation of the delivery vectors into the tumor is a well-accepted phenomenon in preclinical studies but has not yet been confirmed in clinical settings. Additionally, a majority of diseases show a complex microenvironment consisting of diseased cells, tissue interstitium, immune cells and other structural cells of the tissue that limits the ability of the delivery system to access the desired target cells. These physical and physiological barriers further impede the optimal performance of these delivery systems. In the case of cancer, heterogeneity at the cellular and physiological levels significantly limits the ability of these vectors to access their targets. A majority of the stimuli-responsive systems discussed have been tested *in vitro* but few have *in vivo* applications, an aspect that needs immediate focus. The goal is to design simplified systems with positive stimuli-responsive characteristics. This achievement will drastically improve the chances for clinical applications. Though several major hurdles are yet to be overcome, stimuli-responsive systems have ultimately shown tremendous promise as alternatives to the existing delivery approaches.

References

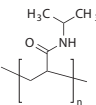
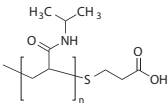
- 1) Iyer, A.K.; Singh, A.; Ganta, S.; Amiji, M.M. Role of integrated cancer nanomedicine in overcoming drug resistance. *Advanced drug delivery reviews* **2013**, *65*, (13–14), 1784–802.
- 2) Meacham, C.E.; Morrison, S.J. Tumour heterogeneity and cancer cell plasticity. *Nature* **2013**, *501*, (7467), 328–37.
- 3) Ganta, S.; Devalapally, H.; Shahiwala, A.; Amiji, M. A review of stimuli-responsive nanocarriers for drug and gene delivery. *Journal of controlled release* **2008**, *126*, (3), 187–204.
- 4) Talekar, M.; Boreddy, S.R.; Singh, A.; Amiji, M. Tumor aerobic glycolysis: new insights into therapeutic strategies with targeted delivery. *Expert opinion on biological therapy* **2014**.
- 5) Devalapally, H.; Shenoy, D.; Little, S.; Langer, R.; Amiji, M. Poly(ethylene oxide)-modified poly(beta-amino ester) nanoparticles as a pH-sensitive system for tumor-targeted delivery of hydrophobic drugs: part 3. Therapeutic efficacy and safety studies in ovarian cancer xenograft model. *Cancer chemotherapy and pharmacology* **2007**, *59*, (4), 477–84.

- (6) Shenoy, D.; Little, S.; Langer, R.; Amiji, M. Poly(ethylene oxide)-modified poly(beta-amino ester) nanoparticles as a pH-sensitive system for tumor-targeted delivery of hydrophobic drugs: part 2. In vivo distribution and tumor localization studies. *Pharmaceutical research* **2005**, *22*, (12), 2107–14.
- (7) Shenoy, D.; Little, S.; Langer, R.; Amiji, M. Poly(ethylene oxide)-modified poly(beta-amino ester) nanoparticles as a pH-sensitive system for tumor-targeted delivery of hydrophobic drugs. 1. In vitro evaluations. *Molecular pharmaceutics* **2005**, *2*, (5), 357–66.
- (8) Gao, W.; Chan, J.M.; Farokhzad, O.C. pH-Responsive nanoparticles for drug delivery. *Molecular pharmaceutics* **2010**, *7*, (6), 1913–20.
- (9) Convertine, A.J.; Diab, C.; Prieve, M.; Paschal, A.; Hoffman, A.S.; Johnson, P.H.; Stayton, P.S. pH-Responsive Polymeric Micelle Carriers for siRNA Drugs. *Biomacromolecules* **2010**, *11*, (11), 2904–11.
- (10) Cheng, R.; Feng, F.; Meng, F.; Deng, C.; Feijen, J.; Zhong, Z. Glutathione-responsive nano-vehicles as a promising platform for targeted intracellular drug and gene delivery. *Journal of controlled release* **2011**, *152*, (1), 2–12.
- (11) Xu, J.; Singh, A.; Amiji, M.M. Redox-responsive targeted gelatin nanoparticles for delivery of combination wt-p53 expressing plasmid DNA and gemcitabine in the treatment of pancreatic cancer. *BMC cancer* **2014**, *14*, 75.
- (12) Kommareddy, S.; Amiji, M. Antiangiogenic gene therapy with systemically administered sFlt-1 plasmid DNA in engineered gelatin-based nanovectors. *Cancer gene therapy* **2007**, *14*, (5), 488–98.
- (13) Egeblad, M.; Werb, Z. New functions for the matrix metalloproteinases in cancer progression. *Nature reviews. Cancer* **2002**, *2*, (3), 161–74.
- (14) Zhang, X.X.; Eden, H.S.; Chen, X. Peptides in cancer nanomedicine: drug carriers, targeting ligands and protease substrates. *Journal of controlled release* **2012**, *159*, (1), 2–13.
- (15) Basel, M.T.; Shrestha, T.B.; Troyer, D.L.; Bossmann, S.H. Protease-sensitive, polymer-caged liposomes: a method for making highly targeted liposomes using triggered release. *ACS nano* **2011**, *5*, (3), 2162–75.
- (16) Schmaljohann, D. Thermo- and pH-responsive polymers in drug delivery. *Advanced drug delivery reviews* **2006**, *58*, (15), 1655–70.
- (17) Jiang, J.; Tong, X.; Zhao, Y. A new design for light-breakable polymer micelles. *Journal of the American Chemical Society* **2005**, *127*, (23), 8290–1.
- (18) Kang, H.; Trondoli, A.C.; Zhu, G.; Chen, Y.; Chang, Y.J.; Liu, H.; Huang, Y.F.; Zhang, X.; Tan, W. Near-infrared light-responsive core-shell nanogels for targeted drug delivery. *ACS nano* **2011**, *5*, (6), 5094–9.
- (19) Hribar, K.C.; Lee, M.H.; Lee, D.; Burdick, J.A. Enhanced release of small molecules from near-infrared light responsive polymer-nanorod composites. *ACS nano* **2011**, *5*, (4), 2948–56.
- (20) Hernot, S.; Klibanov, A.L. Microbubbles in ultrasound-triggered drug and gene delivery. *Advanced drug delivery reviews* **2008**, *60*, (10), 1153–66.
- (21) De Temmerman, M.L.; Dewitte, H.; Vandenbroucke, R.E.; Lucas, B.; Libert, C.; Demeester, J.; De Smedt, S.C.; Lentacker, I.; Rejman, J. mRNA-Lipoplex loaded microbubble contrast agents for ultrasound-assisted transfection of dendritic cells. *Biomaterials* **2011**, *32*, (34), 9128–35.
- (22) Purushotham, S.; Chang, P.E.; Rumpel, H.; Kee, I.H.; Ng, R.T.; Chow, P.K.; Tan, C.K.; Ramanujan, R.V. Thermoresponsive core-shell magnetic nanoparticles for combined modalities of cancer therapy. *Nanotechnology* **2009**, *20*, (30), 305101.
- (23) Majewski, A.P.; Schallon, A.; Jerome, V.; Freitag, R.; Muller, A.H.; Schmalz, H. Dual-responsive magnetic core-shell nanoparticles for nonviral gene delivery and cell separation. *Biomacromolecules* **2012**, *13*, (3), 857–66.
- (24) Cheng, R.; Meng, F.; Deng, C.; Klok, H.A.; Zhong, Z. Dual and multi-stimuli responsive polymeric nanoparticles for programmed site-specific drug delivery. *Biomaterials* **2013**, *34*, (14), 3647–57.
- (25) Ge, J.; Neofytou, E.; Cahill, T.J., 3rd; Beygui, R.E.; Zare, R.N. Drug release from electric-field-responsive nanoparticles. *ACS nano* **2012**, *6*, (1), 227–33.
- (26) Zhu, Y.; Liu, H.; Li, F.; Ruan, Q.; Wang, H.; Fujiwara, M.; Wang, L.; Lu, G.Q. Dipolar molecules as impellers achieving electric-field-stimulated release. *Journal of the American Chemical Society* **2010**, *132*, (5), 1450–1.
- (27) Mura, S.; Nicolas, J.; Couvreur, P. Stimuli-responsive nanocarriers for drug delivery. *Nature materials* **2013**, *12*, (11), 991–1003.

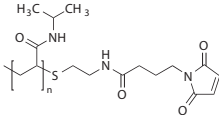
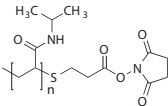
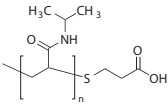
PolyNIPAMs

For more information on this product line, visit aldrich.com/polynipam.

PolyNIPAM

Name	Structure	Molecular Weight	Prod. No.
Poly(<i>N</i> -isopropylacrylamide)		M _w 20,000-40,000	535311-10G
Poly(<i>N</i> -isopropylacrylamide), carboxylic acid terminated		average M _n 10,000	724459-5G

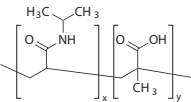
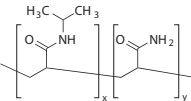
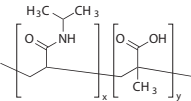
Functionalized PolyNIPAM

Name	Structure	Molecular Weight	Prod. No.
Poly(<i>N</i> -isopropylacrylamide), maleimide terminated		average M _n 2,000	731048-1G 731048-5G
Poly(<i>N</i> -isopropylacrylamide), <i>N</i> -hydroxysuccinimide (NHS) ester terminated		average M _n 2,000	725668-1G 725668-5G
Poly(<i>N</i> -isopropylacrylamide), carboxylic acid terminated		average M _n 5,000	724807-1G 724807-5G

Name	Structure	Molecular Weight	Prod. No.
Poly(<i>N</i> -isopropylacrylamide), amine terminated		M_n 4000-5000	724823-1G 724823-5G
Poly(<i>N</i> -isopropylacrylamide) triethoxysilane terminated		average M_n 2,000-3,000	760978-1G 760978-5G
Poly(<i>N</i> -isopropylacrylamide), maleimide terminated		M_n ~5000	728632-1G 728632-5G
Poly(<i>N</i> -isopropylacrylamide), carboxylic acid terminated		average M_n 7,000	724866-1G 724866-5G
Poly(<i>N</i> -isopropylacrylamide), amine terminated		M_n 7000-8000	724831-1G 724831-5G
Poly(<i>N</i> -isopropylacrylamide), carboxylic acid terminated		average M_n 2,000	724815-1G 724815-5G

PolyNIPAM Copolymers

Name	Structure	Molecular Weight	Prod. No.
Poly(<i>N</i> -isopropylacrylamide-co-butylacrylate)		average M_n 30,000	762881-5G
Poly(<i>N</i> -isopropylacrylamide-co-methacrylic acid-co-octadecyl acrylate)		M_n 30,000-60,000	724475-5G
Poly(<i>N</i> -isopropylacrylamide-co-methacrylic acid)		M_n 30,000-50,000	724467-5G
Poly(<i>N</i> -isopropylacrylamide-co-acrylic acid)		-	741930-5G
Poly(<i>N</i> -isopropylacrylamide-co-acrylamide)		average M_n 20,000-25,000	738735-5G
Poly(<i>N</i> -isopropylacrylamide-co-butylacrylate)		average M_n 30,000	762857-5G

Name	Structure	Molecular Weight	Prod. No.
Poly(<i>N</i> -isopropylacrylamide-co-methacrylic acid)		M_n 60,000	724858-5G
Poly(<i>N</i> -isopropylacrylamide-co-acrylamide)		average M_n 20,000	738727-5G
Poly(<i>N</i> -isopropylacrylamide-co-methacrylic acid)		average M_n 8,000-10,000	750166-5G

WE FOCUS ON MATERIALS

So You Can Focus on Results

Material Matters™ is a quarterly periodical.

- Hot topics in high-tech materials research
- Theme-based technical reviews by leading experts
- Application-focused selections of products and services
- Product application notes



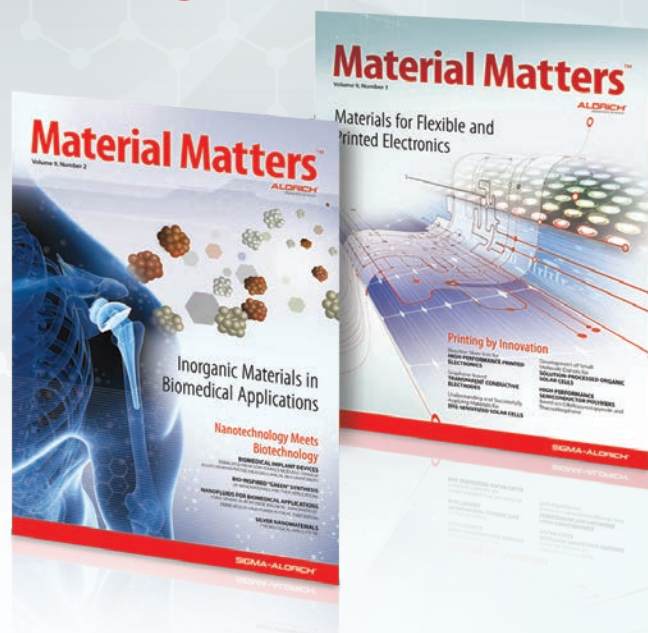
BIOMEDICAL



ELECTRONICS



ENERGY



For a complimentary subscription, visit
aldrich.com/mm

ELECTROSPUN NANOFIBERS

FOR DRUG DELIVERY SYSTEMS



Sang Jin Lee*, James J. Yoo, and Anthony Atala
Wake Forest Institute for Regenerative Medicine, Wake Forest School of Medicine
Medical Center Boulevard, Winston-Salem, NC 27157, USA
*Email: sjlee@wakehealth.edu

Introduction

Local delivery of bioactive molecules using an implantable device can decrease the amount of drug dose required as well as non-target site toxicities compared to oral or systemic drug administration.¹⁻³ Recently, electrospinning techniques using high-voltage electrostatic fields to generate nanofibrous structures have been used to develop drug or protein-loaded electrospun nanofibrous constructs for use as a novel implantable delivery system. The biomimetic cellular environment provided by electrospinning technology resembles the extracellular matrix (ECM) of native tissues and allows for the controlled fabrication of nano- to micro-scale fibers with specific composition, structure, and biomechanical properties of the fibrous constructs.⁴⁻⁸ Recent studies have shown that electrospun fibers with inherently high surface-area-to-volume ratio and high interconnectivity have a number of benefits, including: (1) high drug loading efficiency; (2) the ability to overcome mass transfer limitations associated with most polymeric delivery systems; (3) the facilitation of drug diffusion; and (4) improvement of solubility of various bioactive molecules.⁹ Encapsulation of these bioactive molecules into electrospun fibers allows for localized delivery of antimicrobials, anti-inflammatories, antiscarring agents, antineoplastic agents, immunosuppressives, growth factors, cytokines, genes (DNA and RNA), enzymes, bacteria and viruses, and a number of other important bioactive ingredients to target sites.

Electrospinning Apparatus

Electrospinning has been used extensively to synthesize nanofibers for various applications^{4,6,10-12} because it allows the precise control over the composition, structure, and mechanical properties of the resulting biomaterial. Electrospinning requires a high-voltage power supply, a syringe pump, a polymer solution to be spun, and a grounded collection surface. Polymer solutions are exposed to a high-voltage power supply and delivered with a syringe through a blunt-tip needle using a syringe

pump. Nanofibers can be collected onto a specially designed grounded mandrel placed at a specific distance from the needle tip. Controlling certain variables such as polymer solution concentration, molecular weight, conductivity, surface tension, flow rate, distance, collector geometry, and rotation speed during electrospinning allows for the fabrication of fibers with a specific morphology, diameter, and alignment. The fabricated electrospun nanofibers possess unique features and properties, including an extremely high surface-area-to-volume ratio that enhances cellular interactions with their substrates. The process of electrospinning also allows localized delivery of a combination of bioactive molecules to cells over a prolonged period.¹⁰ Conservation of the structural integrity and bioactivity of the encapsulated drug or protein after the electrospinning process is critical; therefore, several modifications of the electrospinning apparatus are currently being explored to better enable the fabrication of improved drug delivery systems (Figure 1).³

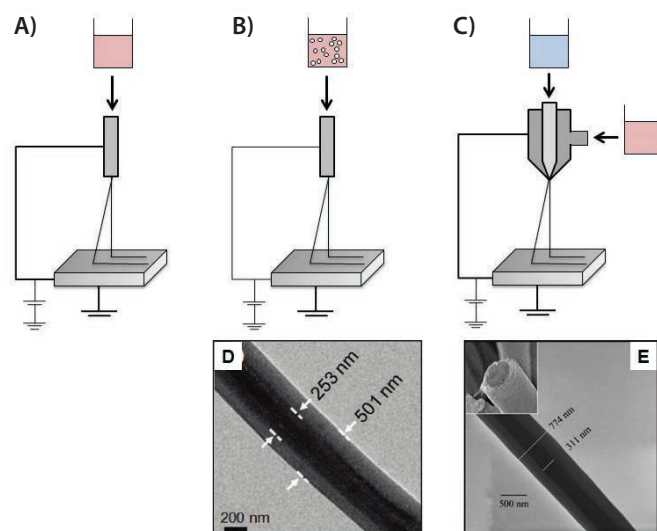


Figure 1. Illustrations of different electrospinning techniques for drug/protein delivery. **A)** Blend electrospinning, **B)** Emulsion electrospinning, **C)** Coaxial electrospinning, **D)** Core-shell structure nanofibers comprised of a poly(vinyl pyrrolidone) (PVP) shell and a polycarbosilane (PCS) core prepared by emulsion electrospinning,¹³ and **E)** Core-shell structure nanofibers composed of a poly(ϵ -caprolactone) (PCL) shell and a bovine serum albumin (BSA)-loaded poly(ethylene glycol) (PEG) core prepared by coaxial electrospinning.¹⁴

Modulation of Controlled Release from Electrospun Nanofibers

Since the release of bioactive molecules occurs primarily by diffusion, it has been demonstrated that the release profile of bioactive molecules from electrospun fibers can be influenced by biodegradability, fiber diameters, hydrophilicity, hydrophobicity, and configuration.¹⁰ In a recent study conducted by our group, electrospun PCL/collagen type I scaffolds derived from calf skin and composed of various fiber diameters were fabricated under conditions in which the concentration of the solution (Figure 2), flow rate, needle diameter, and distance from the substrate were carefully controlled.⁶ The fabricated electrospun PCL/collagen scaffolds showed randomly oriented fibrous structures with a linear relationship between fiber diameter and solution concentration. Distance between dispenser tip, collector, and needle gauge also affected the fiber diameters.

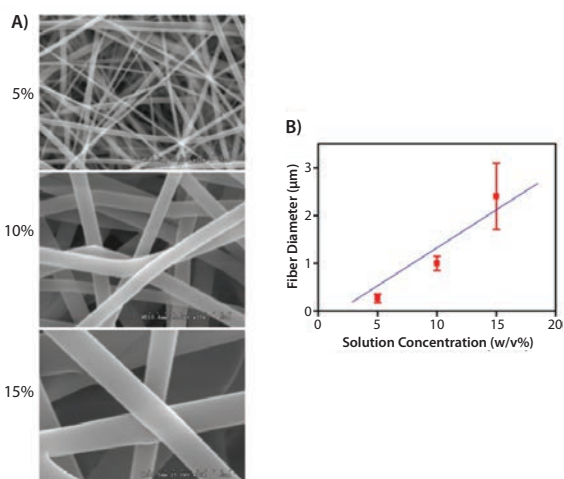


Figure 2. A) SEM images ($\times 10K$ magnification) of electrospun PCL/collagen fibers with different solution concentrations. B) Average fiber diameters of electrospun PCL/collagen fibers depending on solution concentrations.

Okuda et al. demonstrated the release profiles of 5,10,15,20-tetraphenyl-21*H*,23*H*-porphine tetrasulfonic acid disulfuric acid (TPPS)-loaded or chromazural B (ChroB)-loaded electrospun fibers yielded different fiber diameters.¹⁵ For the TPPS-loaded fibers, the sustained release duration and stable quasi-linear release rate were measured as 2 h and 4.0 $\mu\text{g}/\text{cm}^2/\text{h}$, respectively, for smaller fibers (160 nm), and as 4 h and 2.0 $\mu\text{g}/\text{cm}^2/\text{h}$, respectively, for larger fibers (400 nm). Similarly, these parameters of ChroB-loaded fibers were measured as 1 h and 4.8 $\mu\text{g}/\text{cm}^2/\text{h}$, respectively, for smaller fibers (150 nm) and as 3 h and 2.7 $\mu\text{g}/\text{cm}^2/\text{h}$, respectively, for larger fibers (290 nm). Smaller fibers exhibited rapid drug release in the initial stage. Furthermore, no significant differences were observed with respect to the total amount of released drug and the fiber diameter or type of drug. These results demonstrated that the fiber diameter was inversely proportional to the drug release rate and had no measurable impact on the total quantity of drug delivered.

We previously hypothesized that the hydrophilicity of protein-carrier materials can actively influence the extent to which water diffuses through the scaffold, which is directly related to the release kinetics of

the protein released from the scaffolds.¹⁶ In order to achieve controllable delivery of proteins to target locations more efficiently, we developed a novel delivery system based on electrospun fibrous poly(lactide-co-glycolide) (PLGA), with a 75:25 lactide-to-glycolide ratio and molecular weight of 117 kDa, scaffolds combined with variable concentrations of Pluronic® F-127 (PF-127, PEO-PPO-PEO block copolymer (Sigma Prod. No. P2443)). PF-127, an amphiphilic triblock copolymer, provides hydrophilicity to the polymeric scaffolds. Hydrophilic fibrous scaffolds absorb more water; this property may facilitate diffusion of drug or protein molecules from the scaffold. In this experiment, we used BSA (Sigma Prod. No. 05470) and myoglobin (Sigma Prod. No. M5696) as model proteins to study the effects of hydrophilicity on the release of protein from electrospun nanofibrous scaffolds. The addition of PF-127, a hydrophilic polymer, to electrospun fibers significantly increased the initial burst of drug released ($p \leq 0.05$) and caused a subsequent increase in the release rate. *In vitro* release profiles of BSA or myoglobin that were released from the electrospun PLGA nanofibers showed significant variations between fibers with different hydrophilicities ($p \leq 0.05$) (Figure 3)¹⁶.

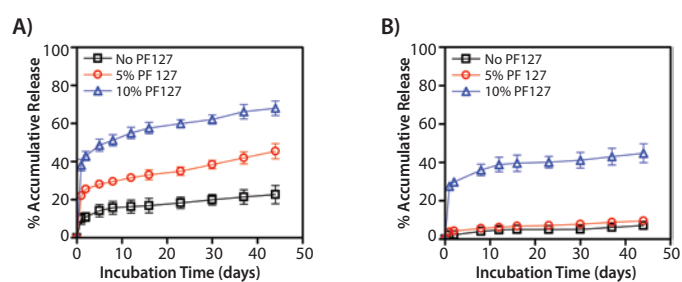


Figure 3. Release profiles of single protein delivery from the electrospun PLGA/PF-127 scaffolds. Percentage of cumulative release of A) BSA and B) myoglobin from electrospun PLGA scaffolds with different concentrations of PF-127. The release of both BSA and myoglobin could be controlled by the scaffold hydrophilicity.¹⁶

Dual Protein Delivery System Using Co-electrospinning

Previous efforts have primarily focused on the delivery of a single bioactive molecule; however, the ability to deliver multiple bioactives with distinct kinetics to drive tissue development to completion is more relevant to the clinical situation.¹⁷⁻²¹ The development of healthy tissues and organs is dependent upon the rapid remodeling of an established vasculature through the coordinated action of many bioactive molecules including growth factors, cytokines, among others.¹⁷ Moreover, sustained release of bioactive molecules with different release kinetics enables effective tissue regeneration,²² which mimics the actual *in vivo* tissue environment during regeneration and contributes to effective and rapid tissue regeneration.^{23,24}

We have developed a novel dual-protein delivery system using electrospun PLGA/PF-127 fibrous scaffolds. These hydrophilic scaffolds have the potential to provide distinct sustained release profiles for multiple proteins. The hydrophilicity of the electrospun PLGA nanofibers can also be adjusted by changing PF-127 concentration during fabrication. Two model proteins, BSA and myoglobin, were incorporated successfully into the electrospun PLGA/PF-127 scaffolds and were released

gradually and in a sustained manner from the scaffolds (Figure 4).¹⁶ Furthermore, the release patterns for these proteins were altered by varying the hydrophilicity of the PLGA/PF-127 composite scaffolds. This co-electrospinning technique can incorporate multiple factors by using two or more syringes and power supplies. It can be used to simultaneously electrospin two or more polymer components (Figure 5). This method has the potential to be an ideal method for the fabrication of smart biomaterial scaffolds for use in the delivery of multiple bioactive molecules in tissue engineering.

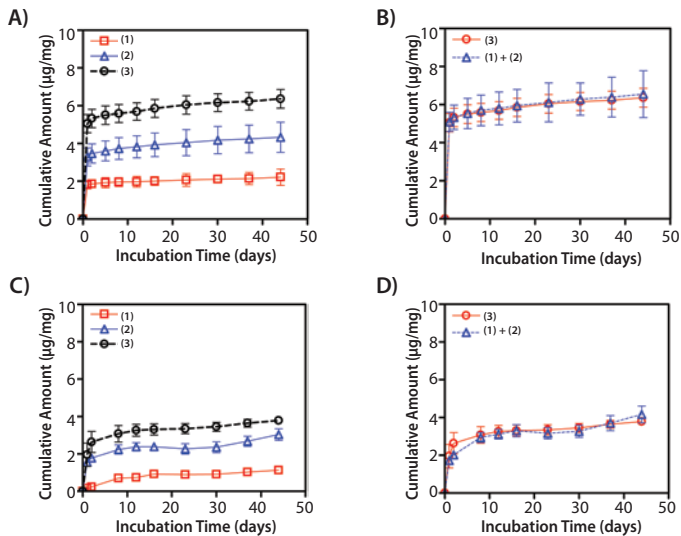


Figure 4. Release profiles of dual protein delivery from the electrospun PLGA/PF-127 scaffolds. Cumulative release amount of BSA (A,B) and myoglobin (C,D) from co-electrospun PLGA/PF-127 scaffolds. 1) PLGA-only + PLGA with 2 wt% protein (BSA or myoglobin); 2) PLGA-only + PLGA/10% PF-127 with 2 wt% protein; and 3) PLGA with 2 wt% protein + PLGA/10% PF-127 with 2 wt% protein (B,D). There was no significant difference between (1) + (2) and (3). This indicates that the co-electrospun scaffolds can deliver multiple factors with the designated release kinetics.¹⁶

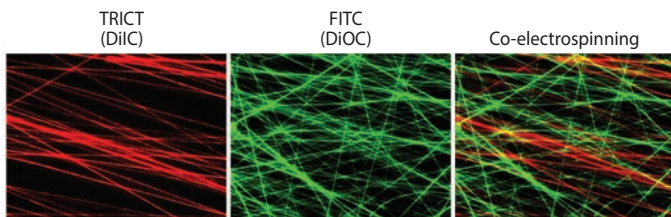


Figure 5. Fluorescent images of functionalized electrospun fibers with incorporating different fluorescence dyes, DiIC (red) and DiOC (green). Co-electrospinning technique showed mixed fibrous structures with red- and green-labeled fibers simultaneously.

Three-dimensional Tissue-engineered Scaffolds

Electrospinning has evolved as a powerful tool in tissue engineering. This fabrication technology provides the ability to control properties such as biomaterial composition, fiber diameter, fiber alignment, geometry, and the degree of drug/protein incorporation in a scaffold. Nanofibers generated by electrospinning can support the adhesion and proliferation of a wide variety of cell types. More importantly, these cells maintain their phenotypic and functional characteristics on these nanofibrous scaffolds.²⁵ Additionally, a number of recent studies have demonstrated that micro- to nano-scaled topography directly affects the adhesion, proliferation, orientation (Figure 6),²⁶ and survival of cells in culture.²⁷ Therefore, studies using electrospun nanofibrous scaffolds can advance our understanding of the topographical aspects of cellular interactions and guide future efforts in regenerative medicine toward improved tissue formation. Furthermore, these scaffolds can be functionalized by adding biochemical and mechanical cues such as surface modification with bioactive molecules to enhance cellular interactions for tissue engineering applications. While specific interactions between cells and functionalized electrospun scaffolds are not fully understood, knowledge gained with respect to the specific modifications that enhance cell adhesion, proliferation, and guidance of cells seeded on a scaffold, as well as those that could affect host cell infiltration, differentiation, and vascularization *in vitro* and *in vivo* will be crucial for the advancement of tissue engineering applications.

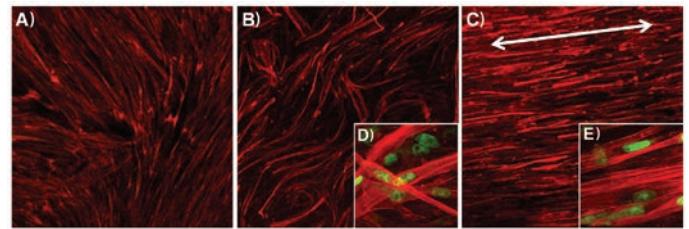


Figure 6. Immunofluorescent images of F-actin of skeletal muscle cells on electrospun PCL/collagen nanofibers: A) culture dish, B) randomly oriented, and C) aligned electrospun nanofibers (x40 magnification). Laser confocal microscopy images of F-actin of skeletal muscle cells seeded on the D) randomly oriented and E) aligned electrospun nanofibers (x600 magnification).²⁶

Conclusions and Future Outlook

Electrospinning has evolved as an important tool in drug/protein delivery by providing the ability to control material composition, fiber diameter, and geometry in order to affect the release profile of bioactive molecules released from electrospun fibers. Bioactive molecules can be incorporated into electrospun fibers using physical adsorption, blend electrospinning, emulsion electrospinning, coaxial electrospinning as well as surface immobilization after electrospinning. Moreover, nano-scaled fiber structures generated by electrospinning can be used to improve cellular interactions, including cell adhesion, proliferation, differentiation, and ECM production allowing the control of scaffold composition, structure, and

mechanical properties. The resulting electrospun nanofibrous scaffolds possess unique features and characteristics, including an extremely high surface-area-to-volume ratio that allows for enhanced cellular activities within the scaffolds. In addition, the high porosity and interconnectivity of the three-dimensional electrospun nanofibrous scaffolds provides a favorable environment for cell infiltration and attachment. The unique characteristics of electrospun nanofibers make these materials a highly promising vehicle for the future delivery of multiple bioactive factors for enhanced drug delivery and tissue engineering applications.

Acknowledgments

We would like to thank Dr. Heather Hatcher for editorial assistance. This study was supported, in part, by the Department of Energy (DE-FG02-09ER64711) and the Telemedicine and Advanced Technology Research Center (TATRC) at the U.S. Army Medical Research and Materiel Command (USAMRMC) through award W81XWH-07-1-0718.

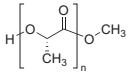
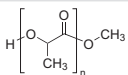
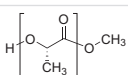
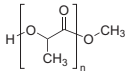
References:

- Laurencin, C.T.; Kumbar, S.G.; Nukavarapu, S.P.; James, R. & Hogan, M.V. *Recent Patents on Biomedical Engineering* **2008**, *1*, 68–78.
- Ashammakhi, N.; Wimpenny, I.; Nikkola, L.; Yang, Y. *Journal of biomedical nanotechnology* **2009**, *5*, 1–19.
- Xu, W.; Lee, S.J. *Recent Patents on Biomedical Engineering* **2012**, *5*, 14–22.
- He, W., et al. *Journal of biomedical materials research. Part A* **2009**, *90*, 205–216.
- He, W.; Yong, T.; Teo, W.E.; Ma, Z.; Ramakrishna, S. *Tissue Eng* **2005**, *11*, 1574–1588.
- Ju, Y.M.; Choi, J.S.; Atala, A.; Yoo, J.J.; Lee, S.J. *Biomaterials* **2010**, *31*, 4313–4321.
- Lee, S.J., et al. *Biomaterials* **2008**, *29*, 2891–2898.
- Lee, S.J.; Yoo, J.J.; Lim, G.J.; Atala, A.; Stitzel, J. *Journal of biomedical materials research. Part A* **2007**, *83*, 999–1008.
- Barnes, C.P.; Sell, S.A.; Boland, E.D.; Simpson, D.G.; Bowlin, G.L. *Advanced drug delivery reviews* **2007**, *59*, 1413–1433.
- Chew, S.; Wen, J.; Yim, E.; Leong, K. *Biomacromolecules* **2005**, 2017–2024.
- Lee, J.; Yoo, J.J.; Atala, A.; Lee, S.J. *Acta Biomater* (in press).
- Pham, Q.P.; Sharma, U.; Mikos, A.G. *Tissue Eng* **2006**, *12*, 1197–1211.
- Choi, S.H.; Youn, D.Y.; Jo, S.M.; Oh, S.G.; Kim, I.D. *ACS Appl Mater Interfaces* **2011**, *3*, 1385–1389.
- Jiang, H., et al. *Journal of controlled release: official journal of the Controlled Release Society* **2005**, *108*, 237–243.
- Okuda, T.; Tominaga, K.; Kidoaki, S. *Journal of controlled release: official journal of the Controlled Release Society* **2010**, *143*, 258–264.
- Xu, W.; Atala, A.; Yoo, J.J.; Lee, S.J. *Biomed Mater* **2013**, *8*, 014104.
- Richardson, T.; Peters, M.; Ennett, A.; Mooney, D. *Nat Biotechnol* **2001**, *19*, 1029–1034.
- Yan, S.; Xiaojiang, L.; Shuiping, L.; Xiumei, M.; Ramakrishna, S. *Colloids Surf B Biointerfaces* **2009**, *73*, 376–381.
- Cheng, D.; Sefton, M. *Tissue Eng Part A* **2009**, *15*, 1929–1939.
- Chapanian, R.; Amsden, B. *Journal of controlled release: official journal of the Controlled Release Society* **2010**, *143*, 53–63.
- Weissman, I.L. *Science* **2000**, *287*, 1442–1446.
- Chen, F.M.; An, Y.; Zhang, R.; Zhang, M. *Journal of controlled release: official journal of the Controlled Release Society* **2011**, *149*, 92–110.
- Borselli, C., et al. *Proceedings of the National Academy of Sciences of the United States of America* **2010**, *107*, 3287–3292.
- Elia, R., et al. *Biomaterials* **2010**, *31*, 4630–4638.
- Lee, S.J.; Yoo, J.J., in *The Handbook of Intelligent Scaffold for Regenerative Medicine*. (ed. G. Khang) 201–218 (Pan Stanford Publishing Pte Ltd, Singapore; **2012**).
- Choi, J.S.; Lee, S.J.; Christ, G.J.; Atala, A.; Yoo, J.J. *Biomaterials* **2008**, *29*, 2899–2906.
- Xie, J., et al., *Biomaterials* **2009**, *30*, 354–362.

Well-defined Biodegradable Polymers

For more information on this product line, visit aldrich.com/biodegradable.

Poly(lactides)

Name	Structure	Molecular Weight	PDI	Degradation Time	Prod. No.
Poly(L-lactide)		average M _n , 10,000	≤ 1.1 PDI	>3 years	765112-5G
		average M _n , 5,000	≤ 1.2 PDI	>3 years	764590-5G
Poly(D,L-lactide)		average M _n , 5,000	≤ 1.1 PDI	<6 months	764612-5G
		average M _n , 10,000	≤ 1.1 PDI	<6 months	764620-5G
Poly(L-lactide)		average M _n , 20,000	≤ 1.1 PDI	>3 years	764698-5G
Poly(D,L-lactide)		average M _n , 20,000	≤ 1.3 PDI	<6 months	767344-5G

End-functionalized Poly(L-lactide)s

Name	Structure	Molecular Weight	PDI	Prod. No.
Poly(L-lactide) 4-cyano-4-[(dodecylsulfanylthiocarbonyl) sulfanyl]pentonate		M_n 10,000	≤ 1.2 PDI	746533-1G
Poly(L-lactide), azide terminated		average M_n 5,000	< 1.2 PDI	774146-1G
Poly(L-lactide), propargyl terminated		average M_n 5,000	≤ 1.1 PDI	774154-1G
Poly(L-lactide), amine terminated		average M_n 2,500	≤ 1.3 PDI	776378-1G 776378-5G
Poly(L-lactide) 2-hydroxyethyl, methacrylate terminated		average M_n 5,500	≤ 1.2 PDI	766577-1G 766577-5G
Poly(L-lactide), 2-bromoisobutyryl terminated		average M_n 10,000	≤ 1.1 PDI	773409-1G
Poly(L-lactide), propargyl terminated		average M_n 2,000	≤ 1.1 PDI	774162-1G
Poly(L-lactide), acrylate terminated		average M_n 5,500	≤ 1.2 PDI	775983-1G
Poly(L-lactide) N-2-hydroxyethylmaleimide terminated		average M_n 5000	< 1.2 PDI	746517-1G 746517-5G
Poly(L-lactide) 4-cyano-4-[(dodecylsulfanylthiocarbonyl) sulfanyl]pentonate		-	-	746525-1G
Poly(L-lactide), thiol terminated		average M_n 5,000	≤ 1.2 PDI	747394-1G 747394-5G
Poly(L-lactide) 2-hydroxyethyl, methacrylate terminated		average M_n 2,000	≤ 1.1 PDI	771473-1G 771473-5G
Poly(L-lactide), acrylate terminated		average M_n 2,500	≤ 1.2 PDI	775991-1G
Poly(L-lactide), 2-bromoisobutyryl terminated		average M_n 5,500	≤ 1.1 PDI	773395-1G
Poly(L-lactide), thiol terminated		average M_n 2,500	≤ 1.2 PDI	747386-1G
Poly(L-lactide) amine terminated		average M_n 4,000	≤ 1.2 PDI	776386-1G 776386-5G

Block Copolymers

Name	Structure	Molecular Weight	PDI	Degradation Time	Prod. No.
Poly(ethylene glycol) methyl ether- <i>block</i> -poly(D,L lactide)		PEG average M_n 2,000 PLA average M_n 2,200 average M_n 4,000 (total)	≤ 1.4 PDI	2-4 weeks	764779-1G
Poly(ethylene glycol) methyl ether- <i>block</i> -poly(lactide-co-glycolide)		PEG average M_n 5,000 PLGA M_n 10,000 average M_n 15,000 (total)	< 1.6 PDI	1-4 weeks	765139-1G
Poly(ethylene glycol) methyl ether- <i>block</i> -poly(D,L lactide)- <i>block</i> -decane		PEG average M_n 2,000 PLA average M_n 2,000 average M_n 4,000 (total)	< 1.3 PDI	2-5 weeks	764736-1G
Poly(lactide-co-glycolide)- <i>block</i> -poly(ethylene glycol)- <i>block</i> -poly(lactide-co-glycolide)		PEG average M_n 1,000 PLGA average M_n 2,200 average M_n (1,100-1,000-1,100)	< 2.0 PDI	2-3 weeks	764817-1G
Poly(lactide-co-caprolactone)- <i>block</i> -poly(ethylene glycol)- <i>block</i> -poly(lactide-co-caprolactone)		PEG average M_n 5,000 (DCM, PEO) PLCL average M_n 5,700 average M_n (1,000-10,000-1,000)	< 1.3 PDI	1-2 months	764833-1G
Poly(lactide-co-glycolide)- <i>block</i> -poly(ethylene glycol)- <i>block</i> -poly(lactide-co-glycolide)		PEG average M_n 1,000 PLGA average M_n 2,000 average M_n (1,000-1,000-1,000)	< 1.2 PDI	1-2 weeks	764787-1G
Poly(ethylene glycol) methyl ether- <i>block</i> -poly(lactide-co-glycolide)		PEG average M_n 5,000 PLGA M_n 55,000 average M_n 60,000 (total)	< 1.2 PDI	1-4 weeks	764752-1G
		PEG average M_n 2,000 PLGA average M_n 15,000 average M_n 17,000 (total)	< 1.8 PDI	1-4 weeks	764760-1G
		PEG M_n 2,000 PLGA M_n 4,000 average M_n 6,000 (total)	< 1.5 PDI	1-4 weeks	764825-1G

CHITOSAN: A VERSATILE PLATFORM FOR PHARMACEUTICAL APPLICATIONS



Raphaël Riva and Christine Jérôme*
Center for Education and Research on Macromolecules
University of Liège, Chemistry Department, Sart-Tilman,
Building B6a, 4000 Liège, Belgium
*Email: c.jerome@ulg.ac.be

Introduction

The development of new medical devices and pharmaceuticals plays an integral role in the medical industry. Both natural and synthetic polymers possess benefits that make them valuable components in therapeutics. In fact, methods to encapsulate drugs in a polymer matrix have demonstrated improved therapeutic efficiency and bioavailability while preventing the drug degradation. In nanomedicine, the development of polymer-based nanocarriers was first initiated in response to the immunologic side reactions encountered with viral-based nanocarriers.^{1,2} In this context, we will discuss the recent emergence of methods that use natural polymers and their derivatives as tools to achieve a high degree of biocompatibility with controlled biodegradability.³

Chitosan for Biomedical Applications

There are several families of natural polymers available on the market. Chitosan is one particular example of a polymer that has been thoroughly studied during the last few decades and shown to be a non-toxic, semi-crystalline,⁴ biodegradable,⁵ and biocompatible⁶ polysaccharide. Chitosan is a random copolymer of *N*-acetyl-glucosamine and glucosamine units obtained by the deacetylation of natural chitin, generally under alkali conditions at relatively high temperature (Figure 1).⁴ Natural chitin is a renewable resource that can be extracted from the exoskeleton of crustaceans or insects. Chitin can also be obtained from non-animal sources, namely from the cell walls of mushrooms.^{7,8} Generally, mushroom-derived chitosan (Aldrich Prod. No. 740500) displays a narrower molar mass distribution, and better traceability and reproducibility compared to chitosan prepared from animal sources.

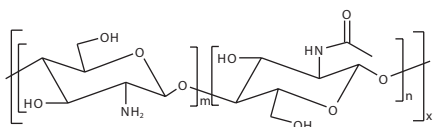


Figure 1. Chemical structure of chitosan.

The demonstrated biocompatibility and biodegradability of chitosan has rapidly paved the way for advancements in a number of biomedical applications⁹ including scaffolds for tissue engineering.¹⁰ For example, the three-dimensional porous structure of chitosan can be seeded with sensitive bioactive agents, including growth factors.¹¹ Additionally, the combined hemostatic¹² and antimicrobial¹³ properties of chitosan make it an outstanding candidate for use in wound dressings.¹⁴⁻¹⁵ In particular, these two intrinsic properties limit the risk of infection which, in turn, improves skin regeneration. The hydrophilic nature of chitosan makes it a suitable starting material for use in biodegradable and biocompatible hydrogels. The mechanical properties of pH-sensitive hydrogels can be adjusted by combining chitosan with simple additives like hydroxyapatite in order to meet specific application requirements.¹⁶

Chitosan for Pharmaceutical Applications

In pharmaceutical applications, chitosan¹⁷ has been successfully applied in the development of drug carriers¹⁸⁻¹⁹ for controlled drug delivery. The presence of positive charges in chitosan has been shown to increase adhesion to mucosa and as a result, increase the retention time.²⁰ The positively charged chitosan backbone also allows for the formation of stable electrostatic complexes with polyanionic macromolecules, such as polyphosphate²¹ or nucleic acids.²² As a result, the application of chitosan for DNA or RNA encapsulation in gene therapy is an area of significant research.²³ Chitosan solubility is of critical importance and is pH dependent. Chitosan is water soluble below pH 6.5 due to the protonation of the primary amine group. When soluble chitosan is required at neutral pH, two possibilities are available; either the use of chitosan oligomers (Aldrich Prod. No. 523682), which are known to be highly soluble in water in a wide range of pH values, or the use of a chemically modified chitosan derivative. Particularly, the ethoxylation of the primary alcohol of both glucosamine and acetyl-glucosamine units leads to *O*-glycol-chitosan, a fully water soluble chitosan derivative.

Chitosan Derivatives for Gene Delivery

Effective non-viral delivery of nucleic acids has many challenges, including degradation via nucleases and a decrease in efficiency due to negative charges accumulated while crossing over cellular membranes. One approach to address these challenges is the formation of polymer complexes, known as polyplexes formed via electrostatic interactions between a polycation and the negatively charged nucleic acid, such as the well-known synthetic non-degradable polyethylenimine. When forming a polyplex with chitosan, the presence of a primary amine group on the glucosamine repeating unit enables control over the charge density. This control is dependent on both the degree of acetylation and the pH. These properties have led to the successful application of chitosan in non-viral gene delivery²⁴ for purposes such as (1) gene

silencing (siRNA, shRNA), (2) compensating for defective genes, and (3) producing beneficial proteins or vaccines (DNA). Chitosan under slightly acidic conditions interacts with nucleic acids such as DNA or siRNA, leading to condensation of the nucleic acids into nanoparticles. This technique was successfully used for the formulation of a siRNA drug delivery system according to an ionic gelation process.²⁵ Additionally, the biocompatibility and low toxicity of chitosan allow it to be used *in vivo*.²⁶ To afford charge permanency and solubility²⁷ in a wider pH range similar to other cationic synthetic polymers such as poly-L-lysine, quaternization of the chitosan primary amine was investigated.²⁸ The quaternary amine was typically generated by reaction with methyl iodide followed by the substitution of the iodide counter-ion with a chloride ion by an ion-exchange process. The resulting *N,N,N*-trimethyl chitosan chloride (TMC) is the most frequently reported quaternized chitosan in the literature used for transfection in gene therapy applications.²⁹ Quaternization of chitosan improved the stability of ionic complexes relative to those based on pure chitosan. Further chitosan derivatizations allowed improvement of the TMC properties. For example, a combination of quaternization and grafting of thiol on TMC yields mucoadhesive properties of TMC by disulfide formation with mucin proteins of the cell membrane.³⁰ Another example is the conversion of some primary amines in chitosan into carboxylic acids by reaction with succinic anhydride, which leads to improved solubility in neutral aqueous media.³¹ The collected acid-bearing chitosan shows a higher solubility into water when at least 20 mol% of the primary amines are converted into carboxylic acids. Despite the fact the stability of the complex of carboxylated chitosan with DNA was shown to be weaker than with pure chitosan, a better transfection efficiency was observed.

The grafting of polymers or functional groups to chitosan is another option to improve gene delivery. The grafting of additional polymers or functional groups can lead to a better solubility and improved buffering capacity compared to unmodified chitosan. For example, the introduction of secondary and tertiary amino groups was shown to improve the transfection efficiency of chitosan.³⁴ This one-step synthesis was based on the grafting of a carboxylic acid-bearing imidazole onto chitosan by amide formation, mediated by 1-ethyl-3-(3-dimethylaminopropyl) carbodiimide (EDC). This simple and reproducible process improved both the solubility and the buffering capacity of the synthesized chitosan derivatives.

Chitosan Derivatives for Drug Delivery

Recent development efforts within the pharmaceutical industry have resulted in a number of highly hydrophobic, and thus poorly water soluble active pharmaceutical ingredient candidates (i.e., BCS Class II and IV drug candidates). This lack of solubility considerably reduces the bioavailability of a drug candidate and complicates its development, preventing commercialization. Targeted nanocarriers can be used to encapsulate hydrophobic drug candidates, allowing for intravenous administration.³⁵ Derivatized chitosan has been shown to be an attractive candidate for hydrophobic drug encapsulation. The grafting of hydrophobic moieties onto the chitosan backbone gave the synthesized polymer amphiphilic properties. This amphiphilic copolymer was shown to self-organize into micelles, with the drug solubilized in the hydrophobic core. Alkyl chains were initially grafted to the chitosan backbone, to form the corresponding Schiff base. This was followed by reduction with NaBH₄.³⁶⁻³⁷ This strategy successfully enabled the grafting of C3, C5, C6, C8, and C12 alkyl chains to chitosan.³⁸⁻⁴⁰ Amphiphilic properties can be more precisely tuned by grafting both hydrophobic

and hydrophilic components on a single chitosan backbone. Sequential grafting of octyl chains by reductive amination followed by the grafting of sulfate was also successfully achieved.⁴¹ The grafting of aromatic rings, namely 2-carboxybenzoyl groups or phthalimide groups, has also been investigated.⁴²⁻⁴³

The use of renewable materials for the modification of chitosan has also been demonstrated. Here, fatty acids were grafted to chitosan using a coupling reaction between the primary amine of chitosan and the carboxylic acid of the fatty acid mediated by EDC in a methanol and water solution.⁴⁴⁻⁴⁵ Using this technique, saturated stearic acid and unsaturated lineoic acid were successfully grafted onto oligochitosan. These derivatives were then modified with cholic acid and cholesterol. Modified glycol-chitosan with 5- β -cholic acid has been extensively studied both *in vivo* and *in vitro* as a carrier for docetaxel and paclitaxel.^{46,47} Similarly, tocopherol-PEG-carboxylic acid has successfully been grafted onto chitosan.⁴⁸

Chitosan can also be modified with synthetic side-chains, particularly with biocompatible and hydrophobic aliphatic polyesters. The grafting of poly(ϵ -caprolactone) (PCL) was largely investigated for the synthesis of amphiphilic biocompatible chitosan based copolymers by both "grafting from" and "grafting to" techniques (Figure 2).⁴⁹⁻⁵⁰ In the "grafting from" technique, the polymerization of ϵ -caprolactone was initiated directly by the primary amine, or the hydroxyl groups, present on the chitosan chain. In the case of the "grafting to" technique, polymer chains bearing an appropriate functional group at one chain-end were grafted onto the primary amine or hydroxyl groups of chitosan.⁵¹

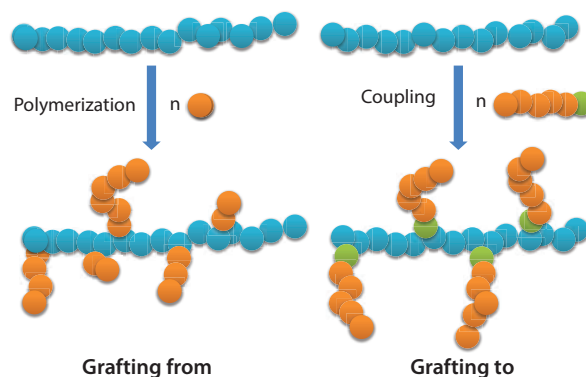


Figure 2. Illustration of the "grafting from" and "grafting to" techniques.

A selective initiation of the polymerization or grafting of a preformed polymer chain, exclusively by the hydroxyl groups can be reached if the primary amines are protected before reaction and deprotected afterwards.^{50,52-53} Remarkably, the chitosan primary amines can be protected by formation of a stable electrostatic complex with methylsulfonic acid, which is easily removed by precipitation in a phosphate buffer after polymerization. The reaction of chitosan with phthalic anhydride is another way to efficiently protect the primary amine groups. Such protection also improves the solubility of chitosan in organic solvents, namely dimethylformamide.⁵⁴ Ester or urethane links are two examples of organic functions used for the grafting of PCL terminated by a carboxylic acid⁵⁵ or an isocyanate group,⁵⁴ respectively, onto hydroxyl groups of phthalimide-chitosan (Figure 3).

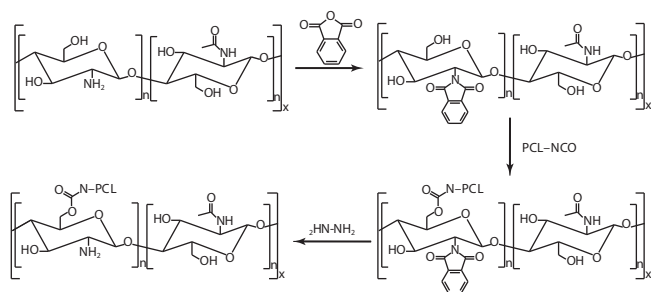


Figure 3. Grafting PCL onto phthalimide-protected chitosan.

Compared to the “grafting from” technique, the “grafting to” technique was shown to demonstrate better control of the number and molecular weight of the PCL grafts onto chitosan. The grafting of polymer chains onto chitosan is not limited to PCL. The grafting of PEG chains onto chitosan is widely described in the literature.^{51,56} Recently, carboxylic acid-terminated PEG chains were grafted onto the primary amines of chitosan. The resulting grafted copolymer showed a reduced cytotoxicity compared to unaltered chitosan.⁵¹ Heterografted chitosan containing both PCL and PEG pendant chains was synthesized by Liu, *et al.* by simultaneous grafting of carboxylic acid-terminated PEG and PCL onto the hydroxyl group of phthalimide-chitosan leading to finely tuned amphiphilic properties.⁵⁷

Finally, glucosamine⁵⁸ (GlcNH₂), the deacetylated monomer unit of chitosan, can be advantageously used to decorate nanoparticles for delivery of antibacterial and anticancer drugs.^{59–60} Indeed, GlcNH₂ is known to be toxic to several malignant cell lines like human hepatoma, prostate, leukemia and breast cancer cells.^{61–64} Hence, GlcNH₂ might be a promising target for the treatment of malignant cancer due to its inhibitory effect on transglutaminase 2 (TGase2), which contributes to drug resistance.⁶² GlcNH₂ has also been used as a ligand in a kidney-targeted drug delivery system for delivery of prednisolone leading to an increase in concentration of prednisolone *in vivo*.⁶⁵

Conclusions

Chitosan has received considerable attention as a functional biopolymer for diverse pharmaceutical and biomedical applications. Chitosan is a nontoxic, biocompatible, and biodegradable polymer. It can be formulated as a nanocarrier using ionic interactions, leading to drug-loaded colloidal systems with mucoadhesive and remarkable permeation-enhancing properties. Additionally, this pH-sensitive polysaccharide can also be formulated as a hydrogel.

The cationic properties of chitosan have enabled its extensive use for gene delivery. While nucleic acid-loaded chitosan nanoparticles fabricated from native chitosan have shown low buffering capacity and limited stability, chemically modified chitosan can help to improve *in vivo* transfection efficiency via: (1) quaternization to improve nanoparticle solubility and stability, (2) grafting of polymer chains to improve endosomal escape, or (3) grafting of ligands for specific cell targeting. When a hydrophobic moiety is conjugated to chitosan, the resulting polymer can self-assemble and encapsulate a poorly soluble drug. Grafting a steroid, fatty acid, or PCL onto chitosan or glycol chitosan can also lead to nanocarriers that are useful for drug delivery, in particular passive or active targeting of anticancer drugs to tumors.

References

- Verma, I.M.; Somia, N. *Nature* **1997**, *389*, (6648), 239–242.
- Rolland, A.; Felgner, P.L. *Advanced Drug Delivery Reviews* **1998**, *30*, (1–3), 1–3.
- Park, J.H.; Saravanakumar, G.; Kim, K.; Kwon, I.C. *Advanced Drug Delivery Reviews* **2010**, *62*, (1), 28–41.
- Rinaudo, M. *Progress in Polymer Science* **2006**, *31*, (7), 603–632.
- Bagheri-Khoulenjani, S.; Taghizadeh, S.M.; Mirzadeh, H. *Carbohydrate Polymers* **2009**, *78*, (4), 773–778.
- Vandevord, P.J.; Matthew, H.W.T.; DeSilva, S.P.; Mayton, L.; Wu, B.; Wooley, P.H. *Journal of Biomedical Materials Research* **2002**, *59*, (3), 585–590.
- Rane, K.D.; Hoover, D.G. *Food Biotechnology* **1993**, *7*, (1), 11–33.
- Arana, I.; Harris, R.; Heras, A. *Current Organic Chemistry* **2010**, *14*, (3), 308–330.
- Croisier, F.; Jérôme, C. *European Polymer Journal*, **2013**, *49*(4) 780–792.
- Madhally, S.V.; Matthew, H.W.T. *Biomaterials* **1999**, *20*, (12), 1133–1142.
- Berscht, P.C.; Nies, B.; Liebendorfer, A.; Kreuter, J. *Biomaterials* **1994**, *15*, (8), 593–600.
- Yang, J.; Tian, F.; Wang, Z.; Wang, Q.; Zeng, Y.J.; Chen, S.Q. *Journal of Biomedical Materials Research Part B-Applied Biomaterials* **2008**, *84B*, (1), 131–137.
- Sudarshan, N.R.; Hoover, D.G.; Knorr, D. *Food Biotechnology* **1992**, *6*, (3), 257–272.
- Tchemtchoua, T.; Atanasova, G.; Aqil, A.; Flee, P.; Garback, N.; Vanhootehem, O.; Deroanne, C.; Noël, A.; Jérôme, C.; Richelle, B.; Poumay, Y.; Colige, A. *Biomacromolecules*, **2011**, *12*, 3194–3204.
- Minagawa, T.; Okamura, Y.; Shigemasa, Y.; Minami, S.; Okamoto, Y. *Carbohydrate Polymers* **2007**, *67*, (4), 640–644.
- Madhumathi, K.; Shalunon, K.T.; Rani, V.V.D.; Tamura, H.; Furuike, T.; Selvamurugan, N.; Nair, S.V.; Jayakumar, R. *International Journal of Biological Macromolecules* **2009**, *45*, (1), 12–15.
- Riva, R.; Ragelle, H.; des Rieux, A.; Duhem, N.; Jérôme, C.; Préat, V. Chitosan and chitosan derivatives in drug delivery and tissue engineering. In R., Jayakumar, M., Prabakaran, & R. A. A., Muzzarelli (Eds.), *Chitosan for Biomaterials II*, Springer, **2011**, 19–44.
- Illum, L. *Pharmaceutical Research* **1998**, *15*, (9), 1326–1331.
- Paños, I.; Niuris, A.; Acosta, H.; Heras, A. *Current Drug Discovery Technologies* **2008**, *5*, 333–341.
- Lehr, C.-M.; Bouwstra, J.A.; Schacht, E.H.; Junginger, H.E. *International Journal of Pharmaceutics* **1992**, *78*, (1–3), 43–48.
- Calvo, P.; Remunan Lopez, C.; VilaJato, J.L.; Alonso, M.J. *Pharmaceutical Research* **1997**, *14*, (10), 1431–1436.
- Lee, K.Y. *Macromolecular Research* **2007**, *15*, (3), 195–201.
- Roy, K.; Mao, H.-Q.; Huang, S.K.; Leong, K.W. *Nat Med* **1999**, *5*, (4), 387–391.
- Mao, S.; Sun, W.; Kissel, T. *Advanced Drug Delivery Reviews* **2010**, *62*, (1), 12–27.
- Ragelle, H.; Riva, R.; Vandermeulen, G.; Naeye, B.; Pourcelle, V.; Le Duff, C.S.; D’Haese, C.; Nysten, B.; Braeckmans, K.; De Smedt, S.C.; Jérôme, C.; Préat, V. *Journal of Controlled Release* **2014**, *176*, (1), 54–63.
- Han, H.D.; Mangala, L.S.; Lee, J.W.; Shahzad, M.M.K.; Kim, H.S.; Shen, D.; Nam, E.; Mora, E.M.; Stone, R.L.; Lu, C.; Lee, S.J.; Roh, J.W.; Nick, A.M.; Lopez-Berestein, G.; Sood, A.K. *Clinical Cancer Research* **2010**, *16*, (15), 3910–3922.
- Verheul, R.J.; Amidi, M.; van der Wal, S.; van Riet, E.; Jiskoot, W.; Hennink, W.E. *Biomaterials* **2008**, *29*, (27), 3642–3649.
- Kotze, A.F.; Thanou, M.M.; Luessen, H.L.; de Boer, B.G.; Verhoef, J.C.; Junginger, H.E. *European Journal of Pharmaceutics and Biopharmaceutics* **1999**, *47*, (3), 269–274.
- Kean, T.; Roth, S.; Thanou, M. *Journal of Controlled Release* **2005**, *103*, (3), 643–653.
- Verheul, R.J.; van der Wal, S.; Hennink, W.E. *Biomacromolecules* **2010**, *11*, (8), 1965–1971.
- Toh, E.K.-W.; Chen, H.-Y.; Lo, Y.-L.; Huang, S.-J.; Wang, L.-F. *Nanotechnology: Nanotechnology, Biology and Medicine* In Press, Uncorrected Proof.
- Jere, D.; Jiang, H.-L.; Kim, Y.-K.; Arote, R.; Choi, Y.-J.; Yun, C.-H.; Cho, M.-H.; Cho, C.-S. *International Journal of Pharmaceutics* **2009**, *378*, (1–2), 194–200.
- Gao, J.-Q.; Zhao, Q.-Q.; Lv, T.-F.; Shuai, W.-P.; Zhou, J.; Tang, G.-P.; Liang, W.-Q.; Tabata, Y.; Hu, Y.-L. *International Journal of Pharmaceutics* **2010**, *387*, (1–2), 286–294.
- Ghosn, B.; Kasturi, S.P.; Roy, K. *Current Topics in Medicinal Chemistry* **2008**, *8*, (4), 331–340.
- Alabadi, H.M.; Mahmud, A.; Sharifabadi, A.D.; Lavasanifar, A. *Journal of Controlled Release* **2005**, *104*, (2), 301–311.
- Ercelen, S.; Zhang, X.; Duportail, G.; Grandfils, C.; Desbrières, J.; Karaeva, S.; Tikhonov, V.; Mély, Y.; Babak, V. *Colloids and Surfaces B: Biointerfaces* **2006**, *51*, (2), 140–148.
- Huo, M.; Zhang, Y.; Zhou, J.; Zou, A.; Yu, D.; Wu, Y.; Li, J.; Li, H. *International Journal of Pharmaceutics* **2010**, *394*, (1–2), 162–173.
- Desbrières, J.; Martinez, C.; Rinaudo, M. *International Journal of Biological Macromolecules* **1996**, *19*, (1), 21–28.
- Rinaudo, M.; Auzely, R.; Vallin, C.; Mullagaliev, I. *Biomacromolecules* **2005**, *6*, (5), 2396–2407.
- Ortona, O.; D’Errico, G.; Mangiapia, G.; Ciccirelli, D. *Carbohydrate Polymers* **2008**, *74*, (1), 16–22.
- Koutroumanis, K.P.; Avgoustakis, K.; Bikiaris, D. *Carbohydrate Polymers* **2010**, *82*, (1), 181–188.
- Bian, F.; Jia, L.; Yu, W.; Liu, M. *Carbohydrate Polymers* **2009**, *76*, (3), 454–459.
- Jiang, G.-B.; Qian, D.; Liao, K.; Wang, H. *Carbohydrate Polymers* **2006**, *66*, (4), 514–520.
- Du, Y.-Z.; Lu, P.; Zhou, J.-P.; Yuan, H.; Hu, F.-Q. *International Journal of Pharmaceutics* **2010**, *391*, (1–2), 260–266.
- Du, Y.-Z.; Wang, L.; Yuan, H.; Hu, F.-Q. *International Journal of Biological Macromolecules* In Press, Corrected Proof.

- (46) Park, K.; Kim, J.H.; Nam, Y.S.; Lee, S.; Nam, H.Y.; Kim, K.; Park, J.H.; Kim, I.S.; Choi, K.; Kim, S.Y.; Kwon, I.C. *Journal of Controlled Release* **2007**, *122*, (3), 305–314.
- (47) Kim, J.-H.; Kim, Y.-S.; Kim, S.; Park, J.H.; Kim, K.; Choi, K.; Chung, H.; Jeong, S.Y.; Park, R.-W.; Kim, I.-S.; Kwon, I.C. *Journal of Controlled Release* **2006**, *111*, (1–2), 228–234.
- (48) Duhem, N.; Rolland, J.; Riva, R.; Guillet, P.; Schumers, J.-M.; Jérôme, C.; Gohy, J.-F.; Préat, V. *International Journal of Pharmaceutics* **2012**, *423*, (2), 452–460.
- (49) Gnanou, Y. *Journal of Macromolecular Science - Reviews in Macromolecular Chemistry and Physics* **1996**, *36*, (1), 77–117.
- (50) Zohuriaan-Mehr, M.J. *Iranian Polymer Journal (English Edition)* **2005**, *14*, (3), 235–265.
- (51) Liu, L.; Chen, L.; Fang, Y.e. *Macromolecular Rapid Communications* **2006**, *27*, (23), 1988–1994.
- (52) Liu, L.; Wang, Y.; Shen, X.; Fang, Y.e. *Biopolymers* **2005**, *78*, (4), 163–170.
- (53) Casettari, L.; Villasaliu, D.; Mantovani, G.; Howdle, S.M.; Stolnik, S.; Illum, L. *Biomacromolecules* **2010**, *11*, (11), 2854–2865.
- (54) Liu, L.; Li, Y.; Liu, H.; Fang, Y.e. *European Polymer Journal* **2004**, *40*, (12), 2739–2744.
- (55) Cai, G.; Jiang, H.; Tu, K.; Wang, L.; Zhu, K. *Macromolecular Bioscience* **2009**, *9*, (3), 256–261.
- (56) Yoksan, R.; Akashi, M.; Hiwatari, K.-i.; Chirachanchai, S. *Biopolymers* **2003**, *69*, (3), 386–390.
- (57) Liu, L.; Xu, X.; Guo, S.; Han, W. *Carbohydrate Polymers* **2009**, *75*, (3), 401–407.
- (58) Boyere, C.; Duhem, N.; Debuigne A.; Pr at, V.; J r me, C.; Riva, R. *Polym. Chem.* **2014**, *5*, 3030–3037
- (59) Veerapandian, M.; Lim, S.K.; Nam, H.M.; Kuppannan, G.; Yun, K.S. *Anal. Bioanal. Chem.* **2010**, *398*, 867.
- (60) Paraskar, A.S.; Soni, S.; Chin, K.T.; Chaudhuri, P.; Muto, K.W.; Berkowitz, J.; Handlogten, M.W.; Alves, N.J.; Bilgicer, B.; Dinulescu, D.M.; Mashelkar, R.A.; Sengupta, S. *Proc.Natl. Acad. Sci. U. S. A.* **2010**, *107*, 12435
- (61) Chesnokov, V.; Sun, C.; Itakura, K. *Cancer Cell Int.* **2009**, *9*, 25
- (62) Kim, D.S.; Park, K.S.; Jeong, K.C.; Lee, B.I.; Lee, C.H.; Kim, S.Y. *Cancer Lett.* **2009**, *273*, 243.
- (63) Zhang, L.; Liu, W.S.; Han, B.Q.; Peng, Y.F.; Wang, D.F. *J. Zhejiang Univ., Sci., B* **2006**, *7*, 608.
- (64) Wang, Z.; Liang, R.; Huang, G.S.; Piao, Y.; Zhang, Y.Q.; Wang, A.Q.; Dong, B.X.; Feng, J.L.; Yang, G.R.; Guo, Y. *Apoptosis* **2006**, *11*, 1851.
- (65) Lin, Y.; Li, Y.; Wang, X.; Gong, T.; Zhang, L.; Sun, X. *J. Controlled Release* **2013**, *167*, 148.

Chitosans

For more information on this product line, visit aldrich.com/natural.

High Purity Chitosans (White Mushroom Origin)

Name	Molecular Weight [M _w]	Degree of Acetylation	Prod. No.
Chitosan	110,000-150,000	≤40 mol. %	740500-1G 740500-5G
	60,000-120,000	≤40 mol. %	740063-1G 740063-5G
	140,000-220,000	≤40 mol. %	740179-1G 740179-5G
	40,000-60,000	≤40 mol. %	746134-1G 746134-5G

Chitosans (Animal Origin)

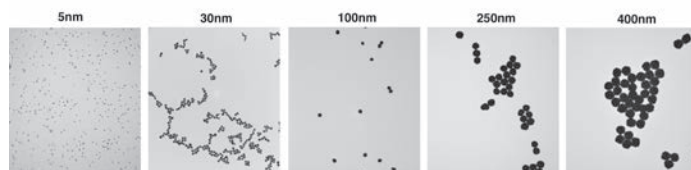
Name	Inherent Viscosity (cP)	Degree of Deacetylation	Prod. No.
Chitosan	20-300 at 25 °C	75-85%	448869-50G 448869-250G
	200-800 at 25 °C	75-85%	448877-50G 448877-250G
	800-2000 at 25 °C	>75%	419419-50G 419419-250G
	>200 at 20 °C	≥ 75%	417963-25G 417963-100G
Chitosan oligosaccharide lactate	-	> 90%	523682-1G 523682-10G

FUNCTIONALIZED, PEGYLATED GOLD NANOPARTICLES

Enhance Your Imaging

- End-group functionalized
 - Carboxylic acid, amino, biotin for protein conjugation
 - Methoxy for non-binding
- Nanoparticle sizes from 5 nm to 50 nm
- 3 or 5 kDa PEG lengths

To browse new products, visit
aldrich.com/functionalnano



BIOMEDICAL



ELECTRONICS



ENERGY

